Politecnico di Torino

Master of Science in Electronic Engineering

Master Thesis

Challenges Of Organic Quantum Dot Cellular Automata Fabrication

Candidate:

Elvio Pio Reveruzzi

Supervisors:

Prof. Mariagrazia Graziano

Prof. Vitali Metlushko, UIC

Acknowledgements

Firstly, I would like to thank my advisors Prof. Vitali Metlushko and Prof. Mariagrazia Graziano. Without their patience, enthusiasm and immense knowledge this work would not have been possible. Their guidance and suggestions guided me in all the time of research and writing of this thesis.
Beside my advisors, I must express my very profound gratitude to my parents and to my uncle for providing me with deep support and continuous encouragement. This accomplishment would not have been possible without them.
Last but not the least, I would like to thank all my friends, that despite 5000 miles from home, they constantly support me and never let me feel alone.

Contents

Summary

Gordon Moore's prediction has held true from 1965 and it establishes that the density of the transistors inside the integrated circuits doubles every 24 months. This prediction has become a remarkable trend in the electronic world. In 2015, the International Technology Roadmap for Semiconductors announced the probable death of the law in the next decade. The transistors industry is reaching its limits. To overcome this problem, the idea of Quantum Dot Cellular Automata is proposed as the new technology for storage and logic applications. Low power consumption, high density and speed of information propagation are some of the most important advantages of this new technology. In this work the contemporary nano-techniques to provide a physical implementation of this new technology and some limitations in nanofabrication processes will be presented.

Chapter 1

Introduction

1.1 Emerging Technology: QCA

For more than 30 years, the science and technology industry has achieved incredible achievements in the development of electronic size and speed. Known as Moore's law, for a long time this trend has been representing a fundamental rule that predicted that the "number of transistors incorporated in a chip doubles every 24 months" [1]. Field Effect Transistors (FET) and Metal Oxide Semiconductor are the backbone of the present digital technologies. Despite huge improvements in these integrated circuits since 1970, they are still used as a current switch. These are tiny transistors in which current flow is controlled by the electric field. This effect occurs in response to external voltage. When the gate size gets reduced to below 5 nm, it causes power dissipation issues in FETs and makes scaling difficult. The transistors industry is reaching its limits. Computation requires the consumption of energy. As CMOS devices become denser, the power consumption of the system also increases. The electronics industry and scientists are looking for ways to replace CMOS technology for high speed and low power consumption. "To overcome this problem, the idea of Quantum Dot Cellular Automata was first proposed by Lent in 1933" [2]. This technology uses the arrangement of individual electrons to send binary information instead of current and voltage. The discovery of Quantum Dot Cellular Automata (QCA) has opened a lot of opportunities in the field of nanotechnology. As a matter of fact, one of the most limiting factors for advancing the current transistor technology is scalability. As logic devices get smaller in form factor, their speed increases. However, at a gate length of 5 nm, the current technology will fall short. The way to advance computing technology is to depend on nanotechnology instead of CMOS technology. Researchers have made many advances when it comes to QCA. "They could fabricate quantum dots with single charge" [3]. Also, they could align many quantum dots, and create arrays with them while maintaining control of their locations, and closely observe their interactions with each other. "The experiments that have been performed so far were difficult, and not high yielding" [3].
One of the main reasons that QCAs were welcomed is because of their small size. A basic QCA cell is made of six quantum dots positioned at the corners and at the center of the square. Each cell contains two extra electrons, as one electron per dot (only two dots will have extra electrons), that can move around among neighboring dots.

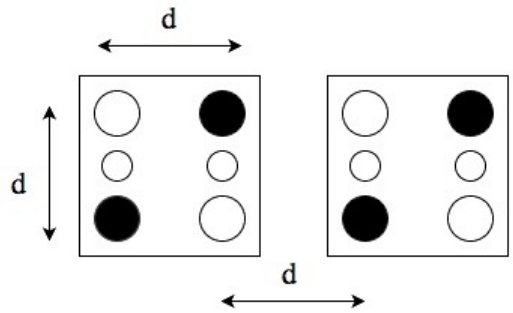

Figure 1.1: Quantum Dot cells structure.

Electrons can move around; However, they cannot leave the cell. A phenomenon called Coulomb repletion (charges that are the same repel each other) causes the settlement of the two electrons on opposite corners of the cell. So practically, "those electrons must assume one of two energetically equivalent ground state polarization configurations" [2]. The two states are labeled as either logic “0” or logic “1”. When two of those cells are brought close to each other, columbus interactions among the electrons in the different cells will cause them to be polarized in the same way. If the polarization of one cell has been switched from one logic configuration to another, the other cell will experience a similar switch to the other stable state. The dots inside the cell are numbered clockwise starting from the top right dot.

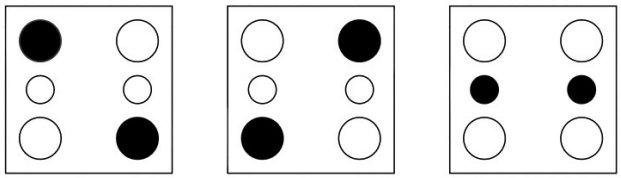

Figure 1.2: Logic configurations of single QCA cell: ‘0’, ‘1’ and ‘NULL’.

For a QCA cell,one of the basic gates is a majority gate. It consists of five cells which are arranged in a cross manner. The cells on the top, bottom, and left act as input cells. As the Coulomb forces of several electrons sum up, so do the middle cells adjust according to the inputs cells. Finally, "the output cell adjusts to the middle cell" [6] and as a result the majority logic value can be obtained from the output cell. The majority gate is the basic logic block in any QCA system.

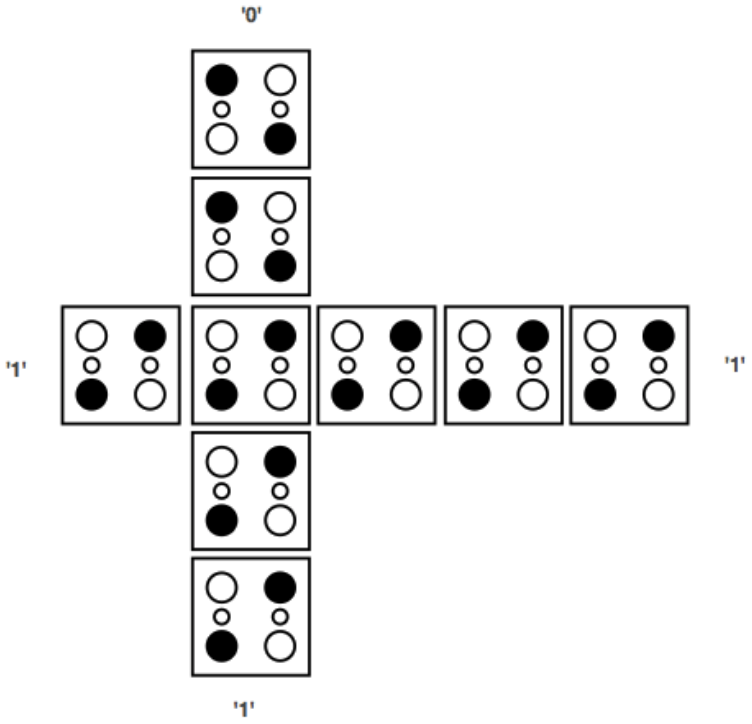

Figure 1.3: Majority gate implemented through QCA cells

It is possible to turn the majority gate into AND-Gate or OR-Gate or NOT-Gate with slight modification. In QCA AND gate, if only one of the inputs of the majority gate is one, the output should not be 1. "A fixed cell is added as a third input that always remain in 0 state. If the two inputs are 1, the two 1s sum up to a stronger Coulomb force than the single fixed 0 cell" [6]. As a result, the majority gate is changed into two input AND gate. The QCA OR gate is built in the same way as AND gate, but instead of fixed 0 a fixed 1 is introduced into the cell. In QCA NOT gate, one QCA wire is forked into two inputs. In this logic gate the output cell is placed next to the forked wires and will settle itself in the opposite configuration respect to the input to reach the minimum energy state.

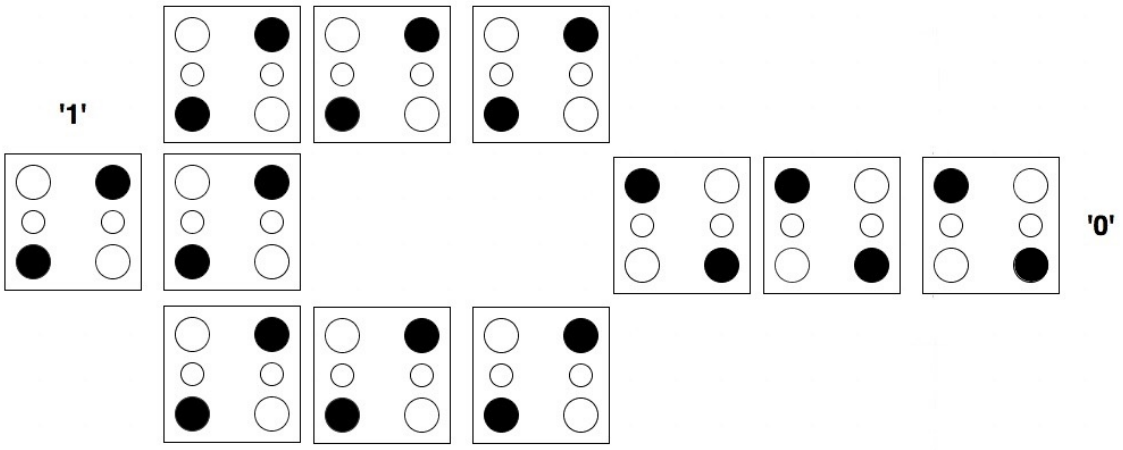

Figure 1.4: QCA Inverter.

The fact that the size of the quantum cells are extremely small has helped the industry to utilize it as a replacement. The ITRS has established that "the size limit for CMOS technology to be around 5 nm to 10 nm, and it is well believed that as of 2016, that limit has been reached already" [5]. By shrinking the size of transistors, researchers could achieve higher speeds, while consuming lower power in the process. However, "as the transistors got scaled down exponentially, they ran into problems of power dissipation, gates leaking current, interconnection noise represented by crosstalk and hot electron effect, in addition to stray capacitances" [4]. All those factors led to a decrease in the overall performance of the circuit. In addition to the form factor, power dissipation has been a major issue with scaling down modern transistors. Specifically, scientists noticed that when the geometry of the transistors is getting smaller, the power density (the amount of energy transferred per unit volume) is increasing tremendously. Therefore, power management becomes an important issue.

1.2 Closk System in QCA Structure

Since there is no current flow between the cells that are neighboring each other, cells interact with each other by mutual interaction. Usually the first cell is called the driver cell (or the input cell), as the state of the driver cell changes, the neighboring cell will change, and so on the other cells in line with the driver cell. This phenomenon (the linear transfer of information without having an actual current or move of charges between cells) allows a line of QCA cells to act as an interconnect between different logic parts of the circuit. There are numerous factors that determine how fast the information will travel down the line. For instance, temperature influences how fast the cells polarize in a specific way. In addition, kink energy (which is defined as the energy that is required to place the adjacent QCA cells in opposite polarization to each other) is an important factor as well. Finally, "quantum relaxation time (defined as the minimum time required for the electrons to overlook their spin direction in which they are oriented) and clock energy (energy from the clock to the signal and vice versa) are important factors as well" [7].
There are groups of logic devices that can be implemented using the property of information transfer between QCA cells. Those logic devices include binary wires, majority gate, and inverters. Starting with the wire, it can be viewed as a series of horizontally placed QCA cells to transmit information from one cell to another. The Fig. 4 here represents a typical QCA wire structure.Specifically, within the QCA cell, the information tends to move in all directions.

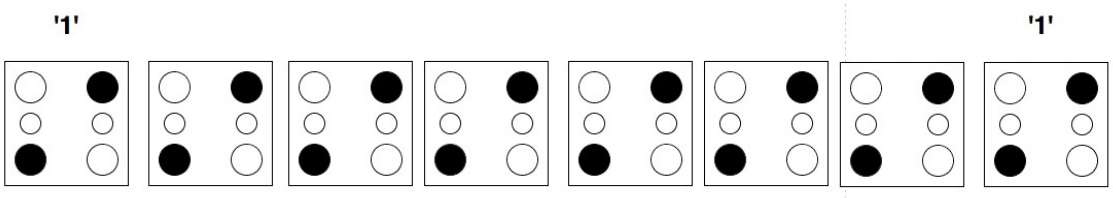

Figure 1.5: Horizontal wire of QCA cells.

Therefore, clocking plays an important role in directing the flow of information in a specific way. Usually the QCA circuit is divided up into a group of clock zones. Clocking, through the application of appropriate voltage,increases and decreases the tunnel barriers between dots for the quantum tunnel effect of the electrons. There are two ways of performing clocking:

zone clocking and continuous clocking. "In zone clocking, a four-phase clocking scheme is introduced to clock each QCA cell" [8]. The clocking mechanism can be imagined as the pump that drives the distribution of data constantly in the QCA cells. Therefore, the structure of QCA cells is always pipelined. "These four phases correspond to switch, hold, release and relax phases" [9]. In the switch phase, the un-polarization of cells begins and the low potential barriers are raised. In the hold phase, the barriers are held high enough so the electrons cannot tunnel anymore, and in the release phase, barriers are lowered down. Thus, the electrons will be free to tunnel again. Continuous clocking, on the other hand, involves the generation of a potential field by a system of embedded electrodes. There are two main types of clocking here, the Landauer clocking, and Bennett clocking. In Launder clocking, the cells have an initial state of null. After the clocking signal is activated, the information will travel from the left to the right. The clocking has two components, a trailer and a header. On one end, the header copies the bit over to the next cell, while the trailer will erase that bit to null. The erasure works toward erasing the copied bit without dissipating energy to the surrounding environment. This opens the door toward a phenomenon that is called reversible computation.

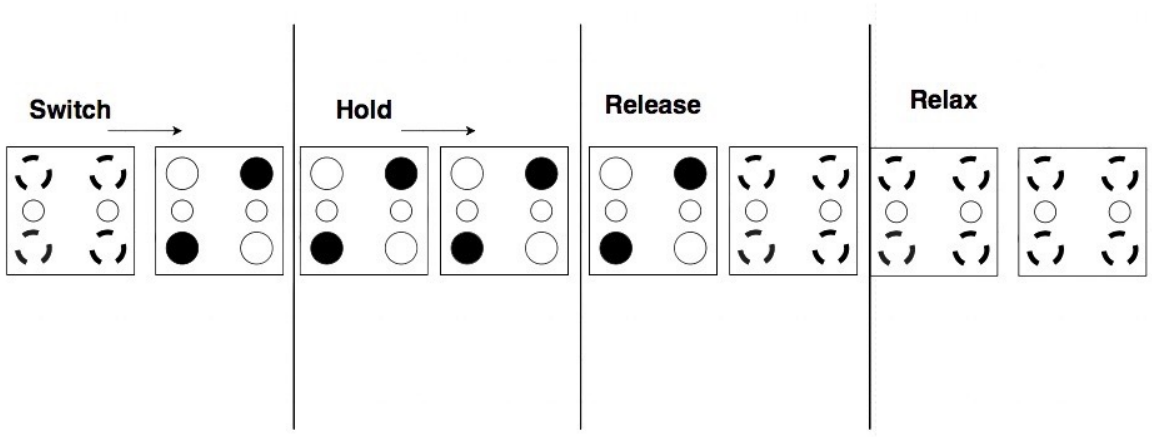

Figure 1.6: Four-phases clock system in a QCA structure.

On the other hand, Bennett clocking works in a different manner compared to Landauer. Basically, the trailer portion of the operation is missing. In other words, cells will still be held in their active states while the information is being passed from the left to the right. An example of this operation is the majority gate. If the clocking method that is utilized is Bennett clocking then the loser in the majority gate within those cells will still be active until the result has been computed. Once the output is finalized, the information will flow to the next stage. And then the clock will start lowering the cells to the null state from the right to the left. One of the major difference between the QCA and CMOS technology.
Basically, with a low clock signal the cell are latched, and with a high clock signal the the electrons will move freely around. The four individual phases are cyclically 90 degrees out of phase with the prior clock phase. This way, two cells will be latched until the next two cells will be latched too. This programmatic way ensures the flow of information is controlled. When the frozen input to the first cell is set to a specific value (either 1 or -1). This clocking zone will serve as an input to the next clocking zone. Therefore, the information will travel down the wire, the next clocking zone will cause the next cell to polarize, and so on. We can assume that after every four-time zone, a new value can be loaded into the QCA wire.
When the signal gets transmitted along a large number of cells within the wire, the signal

tends to deteriorate and this phenomenon is one of the most important challenges of this technology.

1.3 Organic Quantum-Dot Cellular Automata

The field of Quantum-Dot Cellular Automata is on the rise in research due to its promise of decreasing the size for logic gates while also achieving faster computing speed compared to the traditional CMOS technology. For organic QCA, this is done by substituting silicon for organic molecules in such a way that when assembled side-by-side in a cellular fashion the distance between two cells is relatively smaller than the distance between two CMOS transistors. "Information propagation via cellular automata has long been suggested since the 1940s-1950s in the works of pioneering mathematicians such as Von Neumann, Ulam, and Conway" [10]. However, "it is not until 2003 in the truth papers published by Lent and Isaksen from the University of Notre Dame where they suggested using molecules to propagate information via QCA cells in an array" [11]. Before then, ferromagnetic materials were the norm, and along with it came various disadvantages including high power consumption and manufacturing difficulties. Both disadvantages can be eliminated with the use of organic materials.
Snider, et. all's research has proven that "an organic QCA cell can be produced via assembly of biased, vertically oriented, two-dot cells sandwiched between two electrodes and have measured the capacitance of the parallel plate device as a function of applied voltage across the plates" [12]. It has been shown that when propagating the same amount of information as that of the average semiconductor, and depending on the type of molecule used, "organic QCA operates with lesser power consumption and power loss" [12]. This is because information propagation is no longer a function of the current but instead is now dependent on the charge configuration. Research has shown that organic QCA could be operational even at faster clock frequency compared to CMOS transistors which also denotes faster information propagation time [7]. However, unique to each molecule is its own corresponding drawbacks and disadvantages – these will be discussed below.
It is important that we stress the fact that most of these tests have only been done in theory and simulations. So far, no experiment or research has been published primarily due to difficulties in fabrication and anchoring method such that cells are perfectly aligned to maximize electrical interaction among valence electrons on the hybridization cloud. However, it has been suggested that a thin strip of gold film can interact with each organic molecule's thiol, and thus safely anchor and align each cellular automaton.

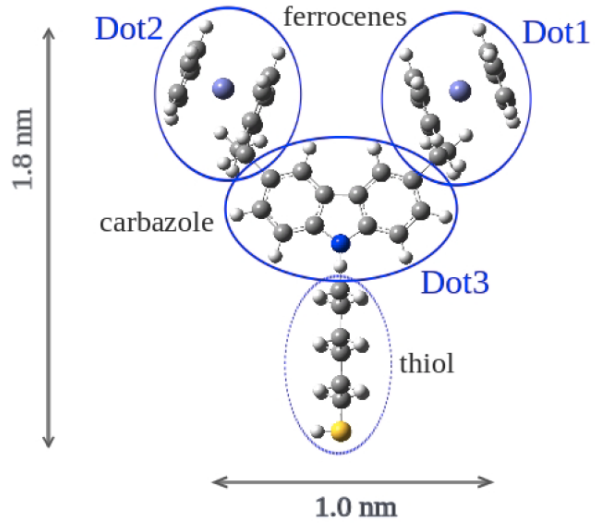

Figure 1.7: Bis-Forrecene molecule structure.
[14]

As of the time of this writing, there seems to be only two molecules presented for QCA implementation: (1) Fe(III)-Ru(II) as proposed by Qi, et. al. [15] and; (2) 'Bis-Ferrocene as proposed by a research group at University of Bologna in collaboration with Polytechnic of Turin and ST Microelectronics company' [13]. Bis-Ferrocene can operate on extremely high frequency transmission even on magnitudes of THz [14]. These molecules allow significantly faster information propagation compared to Fe(III)-Ru(II), and more so when compared to the common CMOS semiconductor. So far, Fe(III)-Ru(II) has only been tested on frequencies of magnitudes in the MHz. Moreover, Fe(III)-Ru(II) propagates information slower than Bis-Ferrocene because electron transfer between metal complex and metal electrode is slow. Furthermore, it was also pointed out that Fe(III)-Ru(II) could only handle voltages of up to 1.0 V. Beyond that degradation to the molecular structure occurs to the point where it can no longer support logic states. There is no research to date pertaining to the voltage tolerance limit for Bis-ferrocene. However, the greatest advantage of Bis-ferrocene over Fe(III)-Ru(II) is the ability of Bis-ferrocene to support a NULL state. By applying the right amount of electric field to the molecule, the electron cloud distribution can be altered in Bis-ferrocene such that the outer electrons are directed inward toward the carbazole region. On the other hand, Fe(III)-Ru(II) cannot support a NULL state. A separate mechanism must be engineered to keep track of a previous state per clock cycle. Subsequent steps should include further research on viable molecular alternatives for organic QCA other than Fe(III)-Ru(II) and Bis-Ferrocene. In our literary research to date, the superior molecule for organic QCA implementation is found to be Bis-Ferrocene. Therefore, we must consider the actual fabrication of Bis-Ferrocene. Additionally, perfect alignment and implantation on the substrate possess an issue in the fabrication of organic QCA cells. Perhaps a unique binding method with the substrate should be put into sincere consideration. Although gold substrate has been found to be functional, gold – or any metal for that matter – has extremely rigid surfaces when talking in the scale of transistors. Due to this, errors in alignment between two molecules is compromised. Perfect alignment is of greatest importance when implementing organic QCA to ensure maximum electron interaction between two molecules, and between two QCA cells.

1.4 Alternative Implementation: Magnetic-QCA

Field-coupled Quantum-dot Cellular Automata is a promising technology for the next generation of computing. It could provide local inter-connectivity for nano-devices. It is especially attractive because it shows the possibility to do dense, high speed, and low power consumption computing. An alternative implementation could be the case of Magnetic QCA that have become promising to form new systems of information transmission based on magnetic dipoles. Magnetic materials are radiation resistant, offer room temperature operation, and offer low power consumption. Furthermore, their fabrication is accomplished using current methods of fabrication. Magnetic QCA uses shapes of nanomagnets that exhibit single domain behavior. Specific type of material and shape anisotropy can be manipulated to orient the direction of the desired ground state using the least amount of energy possible to achieve it. We can see some examples of different nanomagnets shapes with a dominant ground state below.

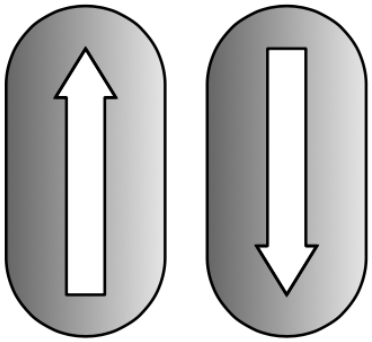

Figure 1.8: Logic configurations of nanomagnets: '1' and '0'.

To build a logic circuit the single nano-magnets should be aligned on the same plane in two possible ways: ferromagnetic or anti-ferromagnetic configuration. This alignment generates the magnetic wire that can be vertical and horizontal respectively if we have a ferromagnetic behavior of the single magnets or anti-ferromagnetic. Interactions between magnets are accomplished through the coupling of spins that creates magnetic dipole moments. Intuitively, "the field interaction between magnetic cells will be affected by the physical dimensions of each magnet" [17]. When information propagates along a wire, each magnet takes the inverted state of its immediate neighbor. This happen thanks to the repulsion forces experienced by similar magnetic poles. The propagation information can propagate in only one direction. To reach it, the logic circuit is subjected to a clock system that works in different phases.

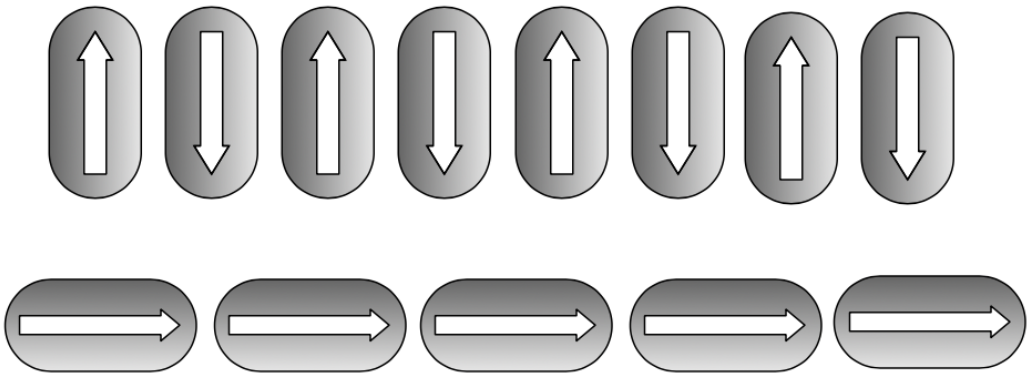

Figure 1.9: Anti-ferromagnetic and ferromagnetic interaction.

As we can see in Fig.10, the tree inputs are switched by using an external magnetic field that unfortunately is not strong enough to switch the other magnets. They require a help that is given by the clock system represented by another magnetic field that aligns all of the magnetization of the single magnets in an unstable configuration to allow them to reorganize like a domino-effect once the magnetic field is removed. The presence of the external magnetic field is of utmost importance for the proper operation of magnetic QCA systems. "A big challenge for magnetic QCA is to obtain the proper step-by-step propagation of digital information across directed paths of a network of bit storage locations without degradation" [18].

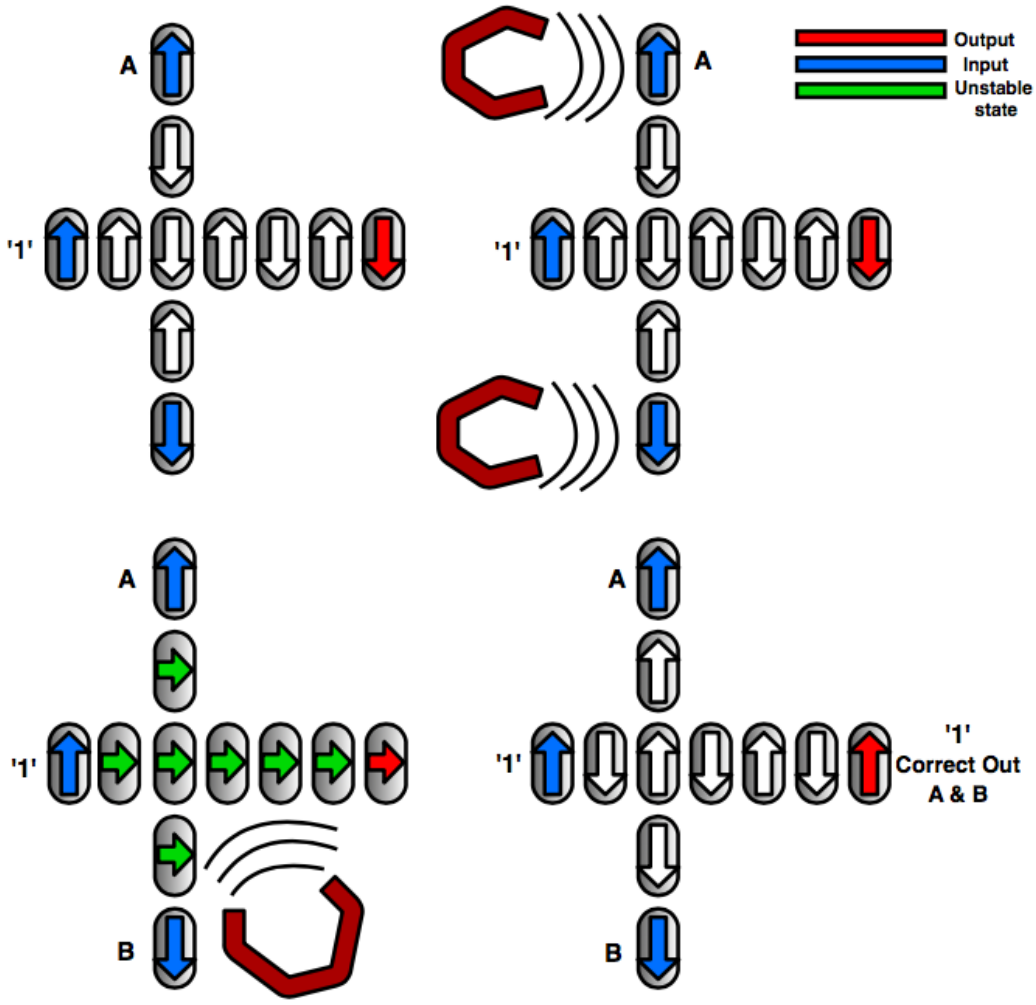

Figure 1.10: Majority gate controlled by a magnetic clock signal.

The requested minimum time for nano-magnets to switch from one configuration to another is limited by their magnetization. Simulations show that at 100 Mhz clock speed power dissipation is improved 2-3 orders of the magnitude over CMOS based systems. "In most computational systems the execution speed of algorithms is severely limited by memory access time" [19]. This emerging technology (NML), therefore represents a very promising opportunity to solve different issues. "Nano-Magnet Logic is the ideal candidate to implement the so-called Logic-In-Memory (LIM) architecture" [18] and to solve the most important problems related to the CMOS technology written before.

Chapter 2

Physiscal Structure of QCA

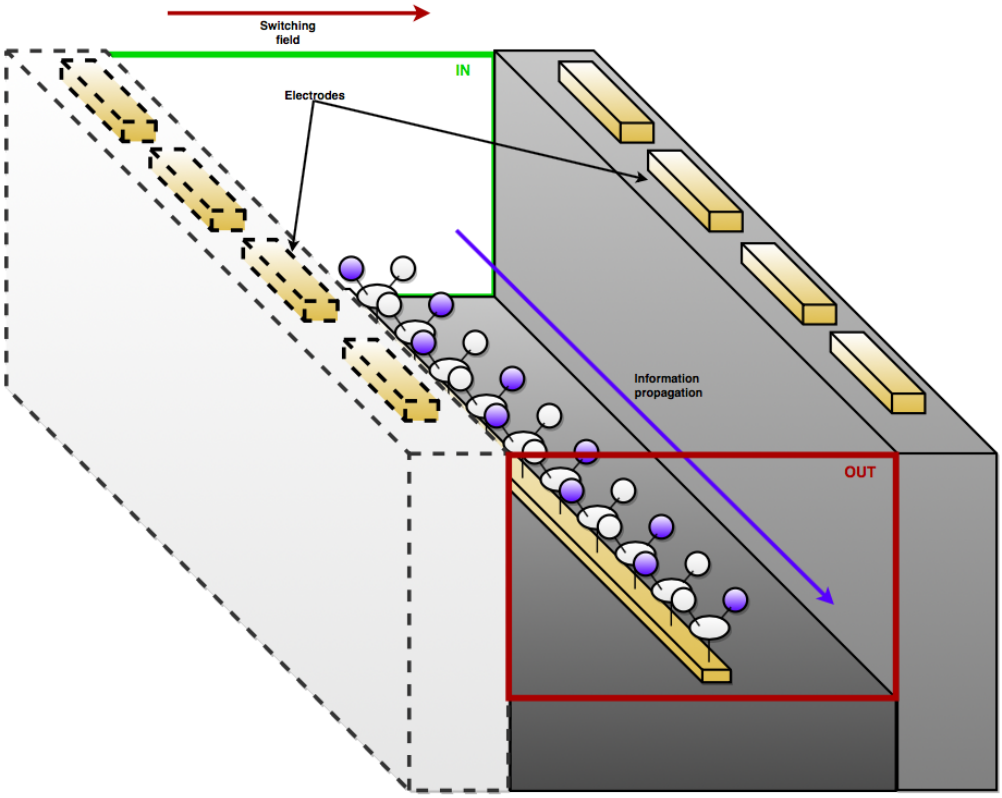

Figure 2.1: Basic structure of single wire of QCA cells with a clock signal.

2.1 Basic Idea

In the previous chapter the general theory of QCA technology was presented, and it was explained how it would be possible to propagate information through the localized charges of the molecules (Bis-Forrecene) positioned on a wire of gold on a silicon substrate. The ideal structure is showed in Fig. 2.1. Placing properly the QCA cells and combining the logic gates (majority voter, inverter, and single wire), it is possible to realize more difficult logic circuits. The wire of nano-gold required for this process can be fabricated through a lithographic process

(EBL) and then an etching process. The molecules of Bis-Forrecene should be positioned on the wire of gold with a self-assembled technique.

2.2 Self-Assembling Technique and Limitations

The nano-fabrication techniques provided today are not enough to set the molecules precisely and individually on a specific substrate. They are too small to be handle and managed. The only solution is to develop a self-assembling process. It is a technique that consist of inserting the nano-structure inside a solution to allow the molecules to attach spontaneously on the surface. As surface, it is possible to use a nanowire of gold because the bottom group of Bis-Forrecene (thiol) attach very well to it. The attachment is divided in two steps: the adhesion of thiol on the substrate and the fastening of three redox centers to the anchoring group.
The molecules should be attached at the same distance to be subjected at the same Columb interaction, but there are important drawbacks that make the implementation of organic QCA technology very difficult. The first problem is related to the fact that not all the molecules will be perfectly horizontal and vertical aligned on the X-Y plane. The second problem is due to the roughness of the surface at nanoscale. The molecules can attach on different parts of the substrate with different high. The vertical displacement of the molecules make worst the interactions between the electrons inside the dots (redox centers) of the molecules altering the propagation of information along the circuit made of QCA cells. Furthermore, it is important to take into account another factor: the torsion of the molecules. As showed in Fig. 1.7 the molecule of Bis-Forrecene presents ideally a Y shape with three different branches. It can happen that the Y shape can be irregular and not well defined due to the mechanical torsion and physical rotation of one or more branches of the molecule.

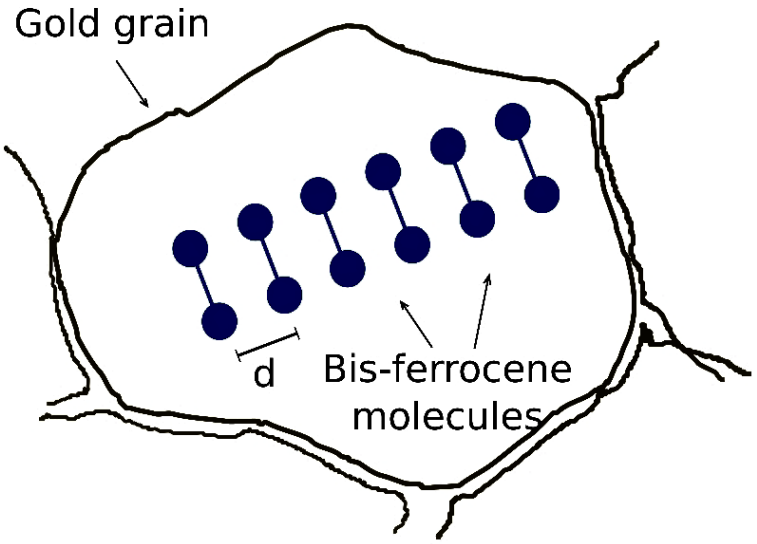

Figure 2.2: Ideal displacement on X-Y plane of the molecules on the substrate of gold. [14]

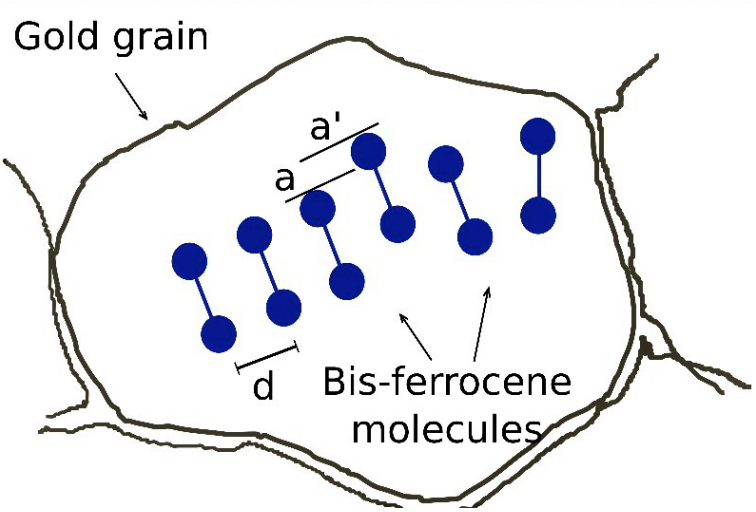

Figure 2.3: X-Y plane misalignment of the molecules on gold substrate. [14]

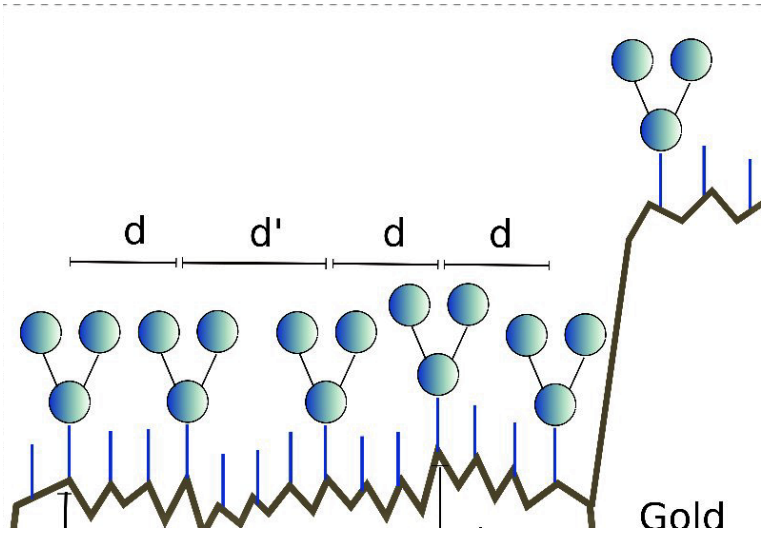

Figure 2.4: Vertical misalignment of the molecules on gold substrate. [14]

2.3 Physical Structure of Organic QCA

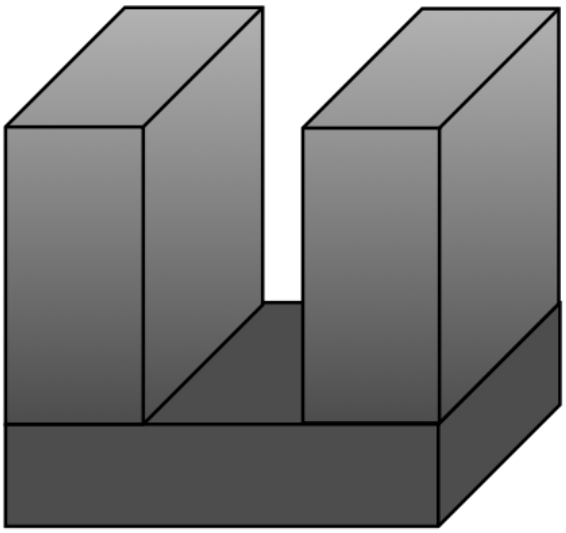

Figure 2.5: Substrate of silicon for m-QCA.

If a realization of logic gates/circuits is wanted, the physical structure should have important characteristics like a substrate that could accept the molecules and a molecule binding method. The first feature of the physical structure is necessary because the position of the molecules on the nano-wire is irregular and difficult to implement. To confine the molecules and the single nano-wire of gold, a physical structure as in Fig. 2.5
'The aspect ratio of this structure must be suitable to bind the molecules inside trench [20]'. The two pieces of semiconductor on the left and right side are needed to place the electrodes on the top for the clock-system of molecular QCA. The four gold-electrodes will provide the correct switching electric field to allow the propagation of information in four phases and in one direction. 'To force the information on the inputs it is possible to implement some drivers' [20].

To create a structure as showed in Fig. 2..6, different micro and nano-fabrication processes are needed:

1) Electron beam or Focused ion beam lithographic process for silicon substrate;
2) Deposition of gold;
3) Electron-beam lithography to realize nano wires of gold and the electrodes;
4) Wet etching/dry etching or lift-off process to take off the excess gold;

EBL or FIB should be used to fabricate the needed trench in the Silicon substrate. In this way, it is possible to continue by depositing a thin film of gold and redefining it subsequently with an etching or lift-off process. Despite the present precise and high resolution technique, there are some limitations and issues that have made m-QCA technology only a theoretical idea, confirmed by simulation but not from a physical point of view. Starting from EBL and continuing with the other fabrication processes, the next stage of this work will be to present

the nano technological processes to make a suitable structure for QCA technology. Considering the limitations due to the used technological techniques, there will be some adjustment and improvement at the structure presented by Polytechnic of Turin.

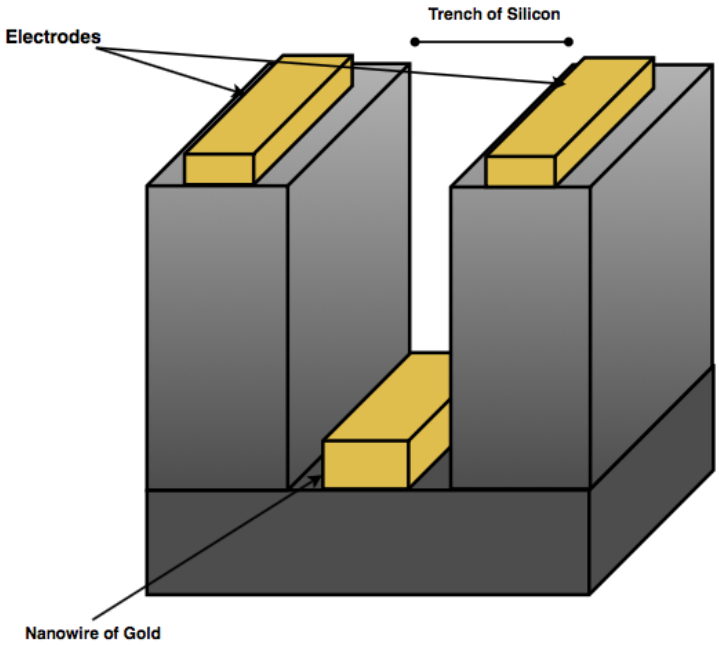

Figure 2.6: Silicon substrate, nano-wire of gold and electrodes.

Chapter 3

Electron Beam Lithography

3.1 Nanofabrication Process for Small Patterns

Semiconductor devices are requiring increasingly smaller size and larger-scale integration. Because of the limited wave length of light, it is not possible to use a conventional photo-lithographic exposure process. In this process a masking material is applied on a photoresist layer that is exposed to irradiated light. However, "there have been various proposed processes, one example of which is an electron beam lithographic process" [21]. EBL is a technological technique used to create nanostructures that are too small to fabricate with a normal photo-lithographic process. It is possible to design the pattern thanks to an electron beam that is scanned over the surface through a series of components like lenses, stigmators, and an electric accelerator. With this technique it is possible to write directly on the surface without using the mask as a protective layer. "The new EBL system is constructed by the insertion of an electrostatic deflector plates system at the electron-beam exit of the column of a scanning electron microscope (SEM)" [22]. "The system can easily be mounted on most standard SEM systems" [22], but is very expensive. In this chapter, the process will be described precisely in every aspect.

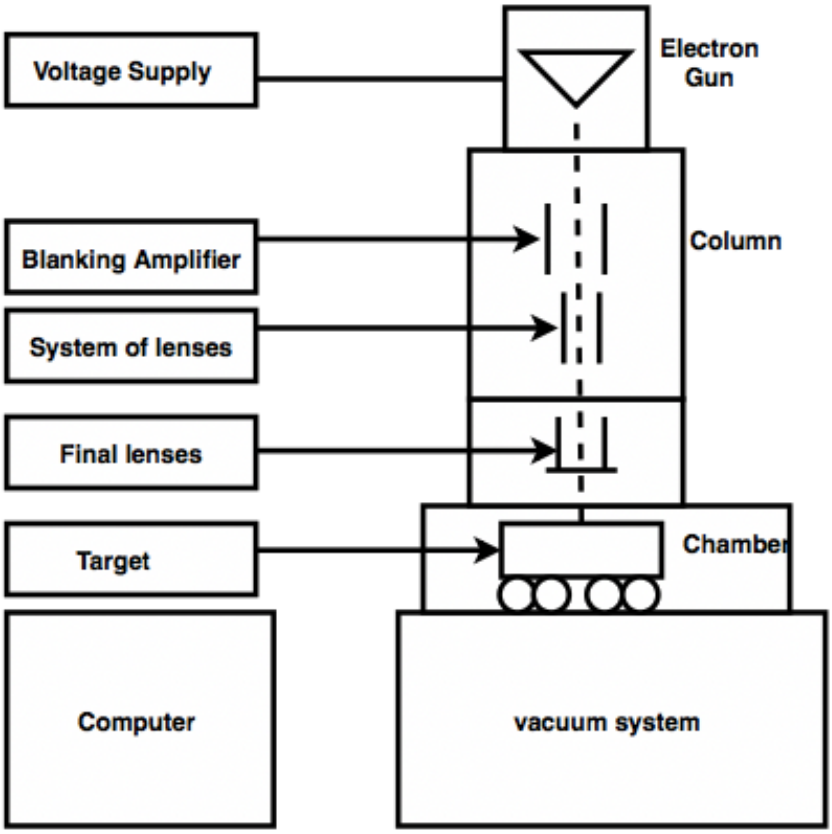

Figure 3.1: EBL system.

3.2 Dual Character of Electron

Electrons can be considered as wave and particle as suggested from the French physicist Louis De Broglie in 1924. According to this theory, small particles when in motion possess wave properties with a wavelength that depends on the mass of the particle that is moving with a certain velocity v and on the Planck's constant (h) that is 6.626 x 10^{34} kgm^2/s.

$$\lambda = \frac{h}{m * v} \tag{3.1}$$

The wave nature of the electron was experimentally showed by Davisson and Germer by observing diffraction effects in an electron beam system. "In 1927, at Bell Labs, Clinton Davisson and Lester Germer fired electrons at a reduced rate against a crystalline nickel target" [16]. The dependence on the incidence angle of the reflected electron was measured, and it was determined that it had the same X-ray diffraction pattern as predicted by William Henry Bragg. The momentum of the particle is defined as the product between the mass and velocity and is related to the amount of energy provided to the electrons when an electric field is applied [23]. The typical applied voltage in an EBL system could be in the rnage of 10-200 kV. Considering the amount of provided energy, the wavelength of the scanned electrons will

be around 0.00251 nm that is less than the other kinds of radiations that are used in normal lithographic techniques. For this reason, this system reaches a higher resolution.

3.3 Electron Gun

"The first requirement for a high-quality beam is a stable, high brightness electron source" [23]. An electron emission involves an amount of energy that should be greater than the work-function of the metal from which the electrons are extrapolated. The work-function of a certain material is defined as the distance between two different energy levels: The Fermi energy level and the vacuum level that is positioned above the minimum of the conduction band. To provide this energy we need to use specific sources that could be thermionic or field emission. In the first case the amount of energy is given to the electrons through the heat. Electrons have an energy related to temperature by the Boltzmann constant (k = 8.617398 x 10-5 eV/K).

$$E = k * T \tag{3.2}$$

Temperature (T) is in Kelvin (K) [24]. A typical thermionic emission source could be a simple wire of tungsten. Its high melting point is the reason why this material is used as an electron source. As a result, it is possible to increase the temperature and help the electron's emission. Because thermionic sources are easy to fabricate, they are widely used today in lithographic systems. The problem of thermionic sources is the generation and emission of the electrons that should operate under vacuum conditions. The equation defines the quantity of the electrons that are emitted from the wire of tungsten is expressed by Richardson-Dashman's law:

$$J = AT^2 e^{-\frac{\phi}{kT}} \tag{3.3}$$

where J is the current density emitted, T the temperature, and ϕ the work-function. For Tungsten, A equals 60 A/cm^2K^2 and the work-function (ϕ) is 4.5 eV. As it is defined by the law, the current depends exponentially on the temperature. The higher the temperature, the higher the current is and the amount of the emitted electrons. The emission can increase until the saturation is reached. The drawback of the wire of tungsten as source is that its lifetime decreases with increasing temperature.
"The quality of the spot is determined by the electron optics, the degree of focus, and the size of the beam" [25]. "It is necessary to have high positional accuracy with limited astigmatism and small spot size" [25]. An important parameter that plays a fundamental role in the size of the beam is the shape of the source. For this reason, the electron thermionic sources are constituted by crystals of lanthanum hexaboride (LaB_6). It is a "refractory ceramic material, insoluble in water, with a low work function and one of the highest electron emissivities known" [26].

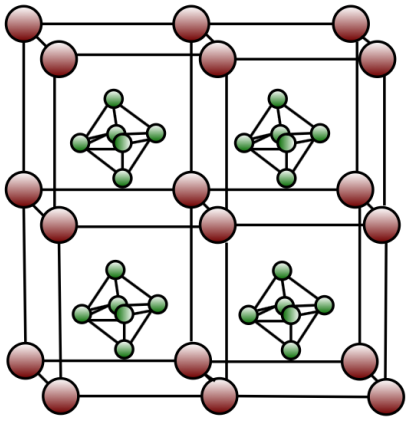

Figure 3.2: Structure of CaB6.

The electrons are accumulated by the Wehnelt cup while they are emitted from the wire of tungsten. The electrons are kept at a minimum voltage of -300 V. The cup is characterized by a small hole where the electrons can pass and can be pulled toward the anode that is part of the electron gun.
Field electron is emission of electrons induced by an electrostatic field that is strong enough to allow the electrons to pass the barrier (work-function) and leave the metal. The sources are usually tungsten tips sharpened to a needle point (possibly the tip of a single atom). "The principle behind FE is that the strength of an electric field E is considerably increased at sharp points" [27] because there is an applied voltage to a (spherical) point of radius r:

$$E = \frac{V}{r} \tag{3.4}$$

Due to the highest electric field reached at the sharpened point, the electron emission location is more controllable. These kinds of sources are called 'Cold' because they usually operate at room temperature. The only disadvantage for this electron source is that the molecules of the sidewalls inside the chamber could covered it. For this reason the emitter should be periodically cleaned. To avoid this situation, "it is more common to use Mueller-emitter-based (TFE – Thermal Field Emission) sources that are operated at elevated temperatures and so considered more stable" [28]. Often TFE sources are tungsten tips coated with zirconium dioxide. The number of emitted electrons can be evaluated through the following equation:

$$J = 6.2 * 10^6 \sqrt{\frac{\mu}{\phi}} \frac{E^2}{\mu + \phi} e^{6.8*10^4 \frac{\phi^{1.5}}{E}} \tag{3.5}$$

Instead of a Wehnelt cup and an anode, the system of electron emission consists of a suppressor and an extractor that operate similarly to the thermionic emission system.

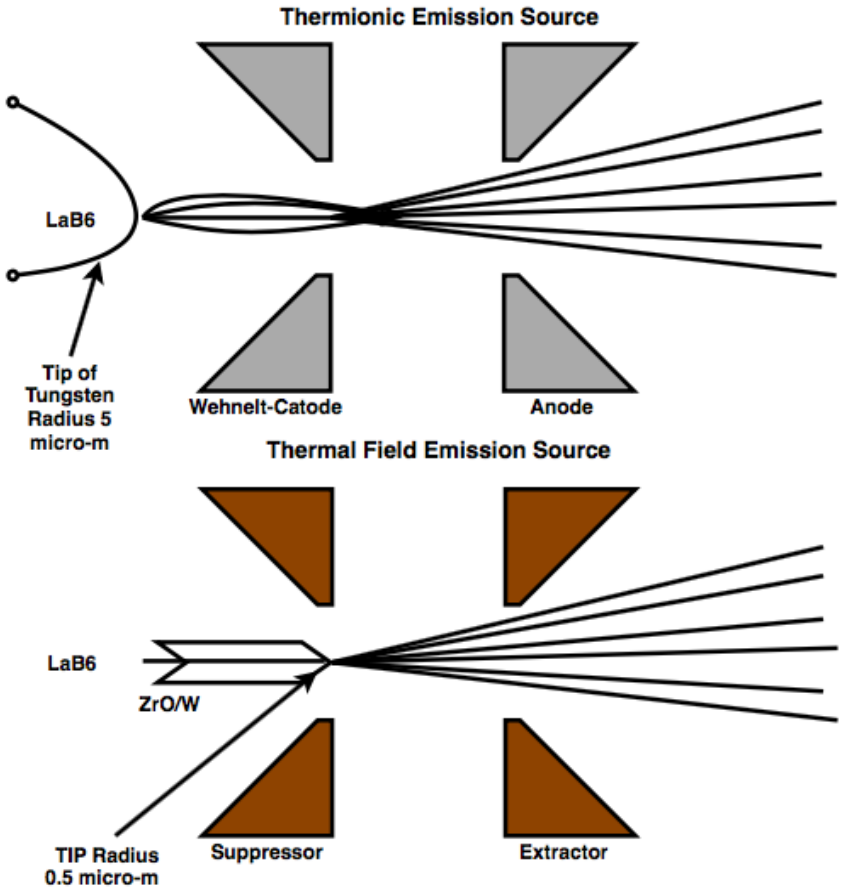

Figure 3.3: Thermionic electron source and TEF electron source.

Type of Source	Brightness ($A/cm^2/sr$)	Size (nm)	Energy Spread (eV)	Vacuum p. (Torr)
Thermionic (W)	10^5	2500	2-3	10^{-5}
Thermionic (LaB_6)	10^6	1000	2-3	10^{-8}
TFE	10^8	20	0.9	10^{-9}
FE	10^9	5	0.22	10^{-10}

Table 3.1: Characteristics of different electron sources.

3.4 Vacuum System

As mentioned before, the vacuum condition is an important requirement for the EBL system. This is because the mass of the electron is very small related to the mass of the other particle, and a collision with a bigger molecule can affect the precision and the resolution of the process. The presence of a vacuum system in EBL defines a further step. Bake-out is a holding step in which the chamber is kept under vacuum and also heated. Heating the walls of the chamber helps the vaporization of the materials and the release of gases that remain in the system.

Because of this, all the equipment inside the chamber should be resistant and compatible with high temperature.

3.5 Acceleration System

After the extrapolation of the electrons from the wire of tungsten the following step is to accelerate the electrons towards the anode (beginning of the electron gun) down the columns to scan the surface. This is possible thanks to the high tension through the electron gun. The EHT (extra-high-tension) should be a perfect trade-off between stability and high energy for the electrons. A higher energy provided to the electrons can cause damages to the surface because the acceleration of the particles is too excessive. At the same time if we want a deep pattern in the working surface a high energy is necessary.

3.6 Electron Deflector and Blanking Process

The electrons, that are pulled towards the surface, generate a beam that scan over the substrate continuously, but a continuous pattern is not always requested. The beam needs to be stopped and restarted. Accelerator and electron gun cannot turn off and turn on quickly, because this means a huge dissipation of energy. To avoid this loss, it is common to use an electrostatic deflector that is made by a pair of plates that are connected to a blanking amplifier with a fast response in time. When the plates are energized the electron beam is deflected from the perpendicular direction respect to the surface. Furthermore, this system allows only the stopping and the starting of the electron beam. "If we want to move it in different directions during the blanking process we should use a different system characterized by an increase number of plates" [29]. In this case, the system will be more precise but the cost of the process will increase dramatically.

3.7 System of Lenses

At the beginning, the generated electron beam is quite divergent and so a system of lenses to focus the rays is necessary. The focus lenses used in EBL system works similarly to the optical lenses, but we have two significant drawbacks: spherical aberration and chromatic aberration. The first phenomenon is related to the different power between the central and the border part of the lenses; the second challenge is due to the electrons characterized by different wavelength and color. Spherical aberration determines a minimum spot size:

$$d_s = \frac{1}{2} C_s \alpha^3 \tag{3.6}$$

that depends on Cs that is a lens constant related to the working distance of the lens [30]. "Spherical aberration makes the probe larger and degrades the beam profile" [32]. To overcome this problem, it is possible to limit the numerical aperture of the probe lens. In EBL system, we can have two different kinds of lenses: electric and magnetic lenses.

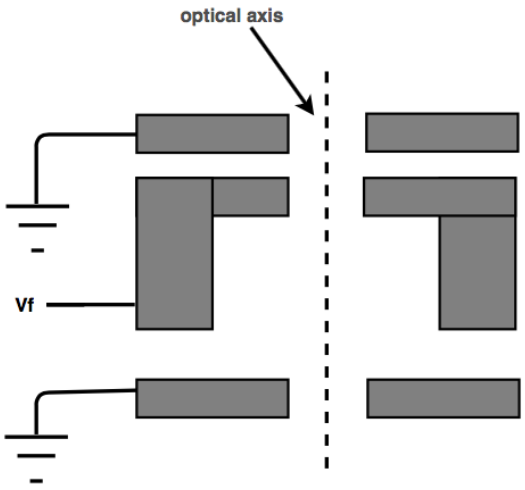

Figure 3.4: Structure of electrostatic lenses.

The electric lenses are not used to focus the beam because they generate more serious aberrations than the magnetic lenses. They are constructed usually near the extractor (anode). The structure of this kind of lens are presented in Fig. 3.4. There are three apertures in series: two at the ground state and one with a variable voltage that control the power of the lenses.
The magnetic lenses are used to focus the beam in a single point. When a magnetic field is applied the particles of the beam are affected by the force of Lorentz:

$$F = q * (v * B) \tag{3.7}$$

where B is the applied magnetic field that comes from the lenses, v is the velocity of the particle and q is the unit charge.

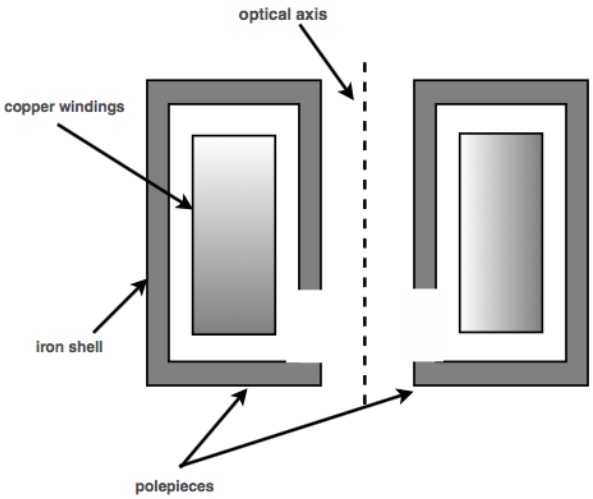

Figure 3.5: Structure of magnetic lenses.

To generate the magnetic field it is possible to use electromagnets that consist of a wire

(usually copper), trapped by a material with high permeability such as iron to encapsulate the magnetic field. A typical structure of the magnetic lenses is shown in the Fig. 3.5.

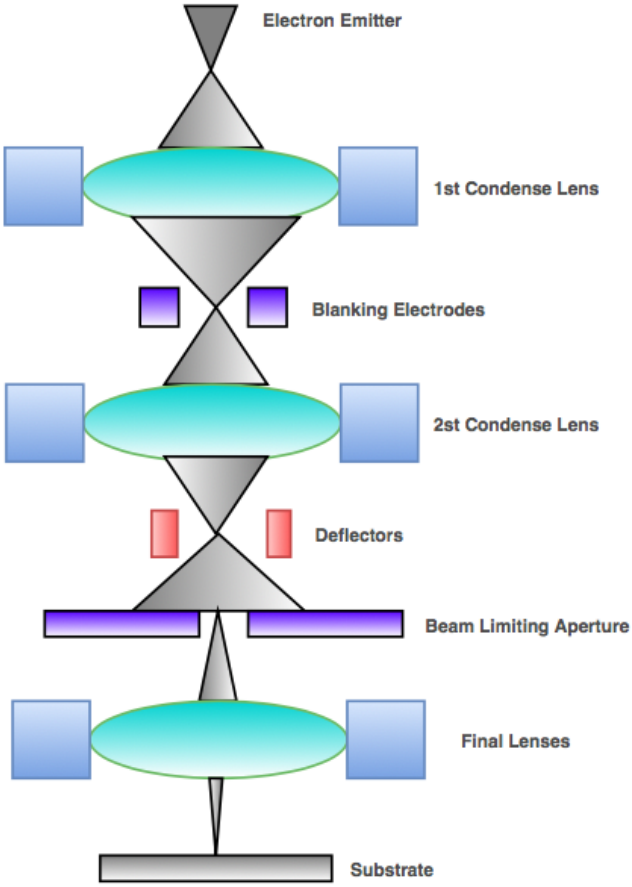

Figure 3.6: EBL multiple system lenses.

With a multiple lenses system it is possible to converge, focus and direct the beam.

1) The condenser lenses are used to converge the electrons that are collected from the source.
2) The intermediate lenses are necessary to direct the beam that comes out from the blanking electrodes.
3) The final lenses focus the beam in one point to pattern the substrate.

3.8 Stigmators

The not perfect shapes of the lenses usually causes a distortion of the circular shape of the electron beam. To avoid this error stigmators are used. They are lenses that compensate the imperfection adjusting the x and y direction of the beam. As the lenses, they could be electric and magnetic.

3.9 Apertures

The Apertures are used to focus the beam and pull out the electrons that are far from the optical axis. The first function is to eliminate the electrons that run with a different wavelength to the others and distort the beam from the original shape. The second function is necessary to modify the shape of the beam in a suitable form (square) to design continuous pattern on the substrate. The size of the aperture defines the amount of the electrons that are scanned over the substrate and the beam current.

3.10 Resist

Resists are generally organic-plastic materials that are used in micro and nanofabrication processes with specific properties. They can be classified in two types: positive and negative. Positive resists are characterized by a solubility that is higher in the exposed regions. Negative resists are characterized by a solubility which is much smaller in the unexposed regions. Below, some resists are described and each one can be used during a lithographic process.
PMMA (Poly-methyl-methacrylate) is a thermoplastic material made of polymers that is used as an alternative resist in respect to the glass. It is a specific material with different properties: it is strong, tough and lightweight with a density of 1.18 g/cm^3, which is less than half of the glass [33]. Developed in 1928 for the first time in Germany, the United Kingdom and Spain it was placed in the market in 1933. Different from SU-8 (epoxy-based negative resist used for photolithography) PMMA (positive resist) has a better resolution that can reach few nanometers (20-30 nm). During the exposure to the beam, the long chains of polymers are fragmented into smaller chains that can be dissolved using a specific solvent as MIBK.
SU-8 2000 is epoxy based photoresist designed for micromachining and nano-electronic applications. SU-8 2000 is an improved formulation of SU-8 that was developed by IBM for the first time, which has been strongly used by MEMS producers for many years especially for UV lithography and X-ray photolithography techniques. SU-8 2000 can produce very high aspect ratio structures and is able to achieve film thickness until 200 microns with only one write process.
ZEP 520A is a high resolution positive electron beam (EB) resist consists of a chain of polymers as other resists. "The molecular weight of this resist is 57,00 and is a solution composed of 11 percent methyl styrene and chloromethyl acrylate copolymer (solid) and 89 % anisole (solvent)" [32]. ZEP520A has been tested with different patterns and has proved to have higher sensitivity than PMMA.
Hydrogen silsequioxane (HSQ) is an excellent tone negative resist for pattern with high resolution. It was showed that it is possible to reach a resolution of 30-20 nm with a layer of thickness of 1 μm.

3.11 Substrate

When a beam of electrons is pulled towards the surface the risk is that the substrate could be charged negatively by the particles. The negative charging of the film causes a further rejection of the electrons due to the repelling force between two particles charged similarly. When the electrons hit the surface of the substrate the amount of energy unleashed should be dissipated quickly through a path to ground. In the EBL process the substrate is a wafer of silicon that easily allows the electrons to follow the path to ground. Sometimes a mask

Resist	Thickness	Developer	Resolution	Rinse	Sensitivity μm/cm2
PMMA	50 nm	MIBK:IPA (1:1)	Low	IPA	150
	60 nm	MIBK:IPA (1:3)	High	IPA	200
ZEP-520A	125 nm	Xylene	Very High	IPA	220
	125 nm	Hexyl Acetate	Very High	IPA	245
HSQ	80	TMAH	High	DI H_2O	300

Table 3.2: Characteristics of different resists.
[31] [33] [34]

is used to help the electrons that are slower than the others in dissipating the energy. The masks in general are made of materials as insulators like quartz.

3.12 Beam Size

The performance of electron-beam lithography (EBL) systems strongly depends on the beam diameter and the current distribution. The first equation we have to take into account that defines the beam diameter when the electrons are pulled out towards the anode inside the gun, is the following one:

$$d_v = \frac{1}{\pi}\sqrt{\frac{i}{\beta}} \tag{3.8}$$

The following phase of the beam is when it comes out from the electron gun with a diameter that is equal to the previous one just multiplied for the Magnification factor:

$$d_g = d_v * M \tag{3.9}$$

where M depends on the convergent angle .
As mentioned before we must consider the two phenomena: Color and spherical aberration.

$$d_s = \frac{1}{2}C_s\alpha^3 \tag{3.10}$$

$$d_c = C_c\alpha\frac{DV}{V_b} \tag{3.11}$$

where DV is the energy of the electrons, Cc is the chromatic coefficient and Vb is the tension of the beam. The last phenomenon that we must consider is the diffraction. To evaluate the diameter due to diffraction effects it is possible to use the following relationship:

$$d_d = 0.61\frac{\lambda}{\alpha} \tag{3.12}$$

where is the wavelength of the electrons. Considering all the effects that we mentioned before the total dimeter of the beam is:

$$d_t = \sqrt{d_g^2 + d_s^2 + d_d^2} \tag{3.13}$$

In EBL systems the total diameter, combining all the effects, is at nm level. The final result is from a theoretical point of view.

3.13 Resolution and Proximity Effect

"Resolution in electron beam lithography is the minimum size of a feature that can be patterned" [35]. "It depends on the type of the resist used, the thickness of the resist, the type of substrate, and the operating conditions" [35]. The pattern is not always so perfect and this is caused by two important phenomena: proximity and scattering. These phenomena depend on how the electrons hit the substrate and interacts with the molecule of the target. When they collide with these molecules of the crystalline structure of the film layer, depending on the interaction, the electrons can keep moving forward or backward. If there is a collision that changes the electron trajectory of a small angle, the movement is forward. In the case of backscatterings the deviation of the trajectory of the electrons that penetrate further into the substrate is larger. The probability of the backscattering phenomena depends on the atomic number of the substrate: high atomic number materials give high backscatterings. These effects cause an increasing of the diameter and a worsening in resolution. The amplitude of the scattered angle depends if the electrons collide with each other or with the nucleus of the molecule of the target (Fig. 3.7).

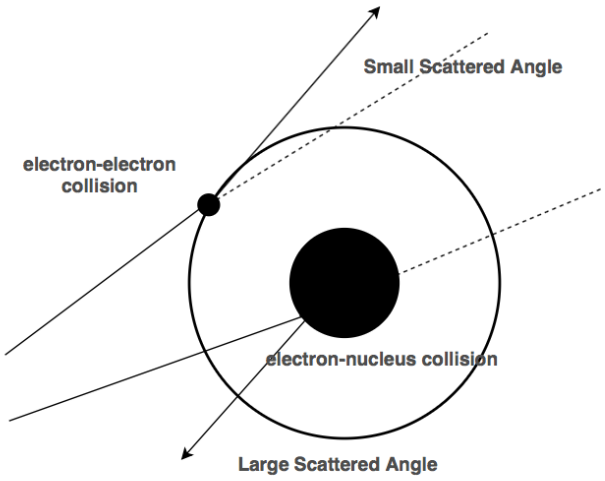

Figure 3.7: Electron-electron collision and electron-nucleus collision.

When two electrons collide, the primary electron exchanges a little amount of energy with the second one changing its initial trajectory. These forward scattered electrons define the major part of the pattern and their contribution for the proximity effect is less than backscattered electrons. The electrons can travel inside the target for a certain distance and this depends on the amount of energy that remains after the collision. As mentioned before, the most important phenomenon for the proximity effect is the collision between the electrons of the beam and the nucleus of the substrate. The transferred energy between the electron and the nucleus is given by the following expression:

$$E = E_0 * \frac{1.01 + \frac{E_0}{10^6}}{465.7A} \tag{3.14}$$

where A is the atomic number of the sample and E_0 is the energy of the beam [36]. If E overcome a certain value, the crystal structure of the target could be damaged. "This

displacement energy changes are related to the materials used as a target: for example, for a diamond the energy to damage the crystal structure is 80 eV" [36].
"The proximity effect is the change in feature size of pattern because of non-uniform exposure in regions adjacent to those addressed by the electron beam" [37] and is a direct consequence of Electron Scattering.

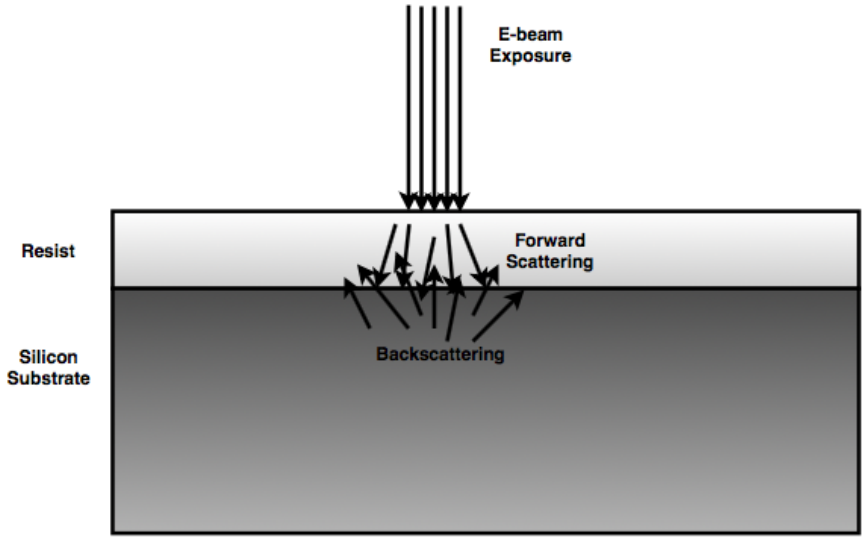

Figure 3.8: Backscatterings and forward scatterings.

An important step during the electron beam lithographic process is to correct the consequences of the proximity effect. The consequences of this phenomenon are the limits on the EBL resolution, the corners of the pattern that becomes rounded and so not well defined, the space that divides continuous patterns,and the not uniform width of the line. We can define two kinds of proximity effect: Intra-proximity and Inter-proximity effect. In the following chapter various PEC methods will be addressed.

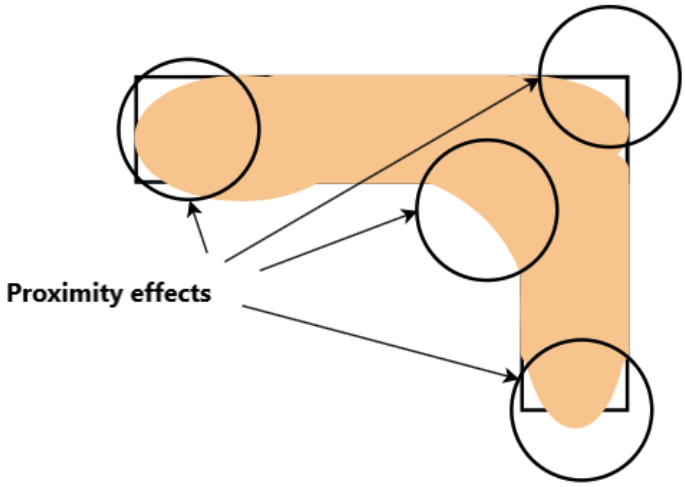

Figure 3.9: Proximity effects on defined pattern (rounded profiles).

Chapter 4

Proximity Effect: How to Correct it?

4.1 Inter-proximity and Intra-proximity Effect for m-QCA

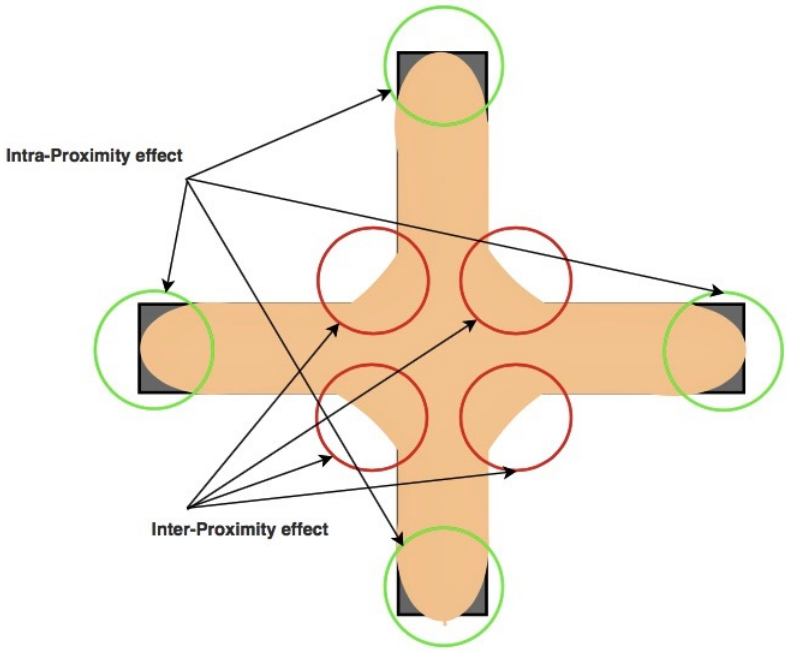

Figure 4.1: Proximity effects at intersection point between two nano-wires of gold.

For the realization of a physical m-QCA system, as written in the second chapter, a nano structure of gold is needed. To fabricate it, a EBL was presented with specific aspects of the process. A drawback of this technique is the proximity effect that can affect the precise shape requested at nanoscale. This happens especially when the pattern on the substrate is characterized by an intersection between two or more nano-wires of gold. One of the most common logic gates theoretical proposed for QCA is the majority gate.
To design a majority gate it is necessary to cross two wires of QCA cells perpendicularly (Fig. 1.3). To define this pattern with an EBL process, we should expose the substrate increasing two times the proximity effect at intersection point.
To overcome this issue, it is possible in two different ways: dose modification and shape

modification. Despite the fact that these physical techniques have effectively reduced the proximity effects, the achievable resolution still remains too low for some nano-structures.

4.2 Quantization of the Proximity Effect

The parameters that allow to quantify the proximity effect are: resist thickness, resist type, exposure time, development time, and electron beam energy. The proximity effect leads an increasing of the beam size that is defined by the following expression:

$$d_{eff} = 0.9(\frac{R_t}{V_b})^{1.5} \tag{4.1}$$

where R_t is the thickness of the resist, d_f if the "effective beam size", and V_b is the voltage provided to scan the beam towards the target. A method that is typically used to quantify the proximity effect is the Modulation Transfer Function. This function is reached by the Fourier transform and the following normalization of the energy density profile:

$$M = \frac{1}{1+\eta}(e^{\frac{-\pi^2\alpha^2}{p^2}} + \eta e^{\frac{-\pi^2\beta^2}{p^2}}) \tag{4.2}$$

where α and β are experimental data, and p is the spatial period [29]. Usually the ideal value of M should be 1, but this for the proximity effect does not happen.

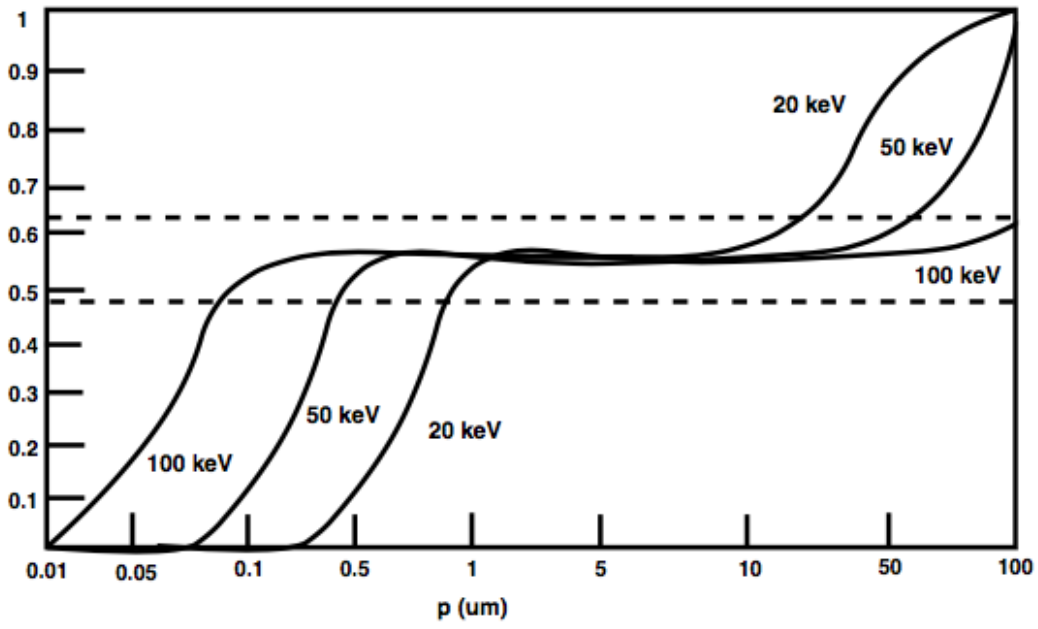

Figure 4.2: "MTF curves for a beam energy of 20, 50 and 100 keV for a Si substrate with 0.5 μm of resist" (34).

As it is possible to see from the Fig. 24 the value of M is not perfect 1 and varies related to the energy beam size. Higher is the energy of the beam and longer is the flat part of the curve. The high energy decreases the sensitivity of the process and it is possible to balance it

by increasing the dose. Although, there are two important risks:

1) the damage of the crystal structure of the substrate;
2) the back-scattered electrons that can easily penetrate reaching the interface resist/substrate;

On the other hand, a low value of energy increases forward scatterings.
Neverthless the energy of the beam size, another important parameter is the thickness of the resist. It depends on how thick the protection layer is and how much small the features of the patterns are. "The ratio between the thickness of the resist and the size of the smallest feature of the pattern should not be very high because different structures of the pattern could be distorted" [38].
The last two parameters, the exposure time and the development time, depends strongly on which kind of resist is used (negative and positive). A positive resist will remain in the un-exposed area while the exposed ones will be etched. Because of further scattering phenomena the shape of the pattern for positive resist should be controlled and eventually corrected with one of PEC methods. Oppositely, the negative resist will remain in the exposed area while the un-exposed ones will be etched. Because of the less scattered electrons the shape of the resist will be more accurate, but despite this, because of its smoothness, a following correction process is necessary.

4.3 Dose Modification

Dose modification technique was developed for the first time in 1978 by Parikh. He provided a method to evaluate and change the amount of doses that could be applied to reduce the proximity effect. The incident dose has to be modified and increased to compensate the forward scattering effects in the resist. The aim is to obtain the identical number of electrons released from the gun and absorbed in the resist. To calculate the dose per each single shape of the pattern is necessary to solve the following system of equations:

$$\begin{cases} E_T = I_{11} * D_1 + I_{12} * D_2 + I_{13} * D_3 + ... + I_{1N} * D_N \\ E_T = I_{21} * D_1 + I_{22} * D_2 + I_{23} * D_3 + ... + I_{2N} * D_N \\ E_T = I_{N1} * D_1 + I_{N2} * D_2 + I_{N3} * D_3 + ... + I_{NN} * D_N \end{cases} \tag{4.3}$$

where N is the number of the shapes, E_T is the required exposure per each shape, $I_{i,j}$ is the proximity interaction between two different shapes (i and j), and D_i is the Dose that has to be calculated. The proximity effect due to the electrons back-scattered at resist/silicon interface could be modulated by a proximity function (PSF). This function defines the distribution of the electrons for each shape when they are scanned on the substrate. To define the interactions between two shapes i and j we need to evaluate the following integral:

$$I_{ij} = \int_{A_i} \int_{A_j} PSF dA_j dA_i \tag{4.4}$$

The integral that defines the proximity interaction between two general irregular shapes is not possible to evaluate analytically. Parkhin derived an expression that calculates the interaction between two rectangular shapes. From this expression, it is possible to evaluate the interaction with any kind of shapes by reducing each of them into a set of rectangles that all together define the original area of the shape. The proximity of the two irregular shapes

will be the sum of the single infinitesimal interaction between the rectangles that repartitioned the shape. After the calculation of the matrix $I_{i,j}$, it is possible to derive the single corrected dose per each shape. "This algorithm provides good corrections for a wide range of feature shapes and sizes using both positive and negative resist" [39].
This correction process does not work perfectly: there are some limitations. It corrects the effect only for exposed areas and not for the uncovered areas because it receives a certain amount of un-desired electrons due to the backscattering effects. To solve this issue, it is important to also calculate the exposure value of the dose, especially at the edges of the shape. To achieve it, "another PEC method was developed for line patterns" [40]. This method defines a specific dose for the edges of the shape that must be equal to E_T (threshold value for the solution of the resist). One of the contemporary approaches to modify the dose is the Critical Dimension Control. This technique is very important because it corrects only long range scatter dose distribution. This technique considers that the short-range scatter is too small in respect to the smallest feature of the pattern. In 1992 another PEC method was developed by Murai et Al. To describe this process, it is crucial to define a parameter: The Pattern Area Density that is the ratio between the exposed area on the total area in the region. The pattern is divided in square meshes with a fixed size and per each square the pattern area density is calculated to obtain the Pattern Area Density Map of the partitioned circuit. By analytically filtering and correcting each calculated density in the single square, it is possible to correct the dose quantity of the beam per the entire pattern. In this process the size of the single mesh is very important because the result of the correction depends on it. Despite that dose modification correction is the most accurate process to modify the pattern scanned and reach the desired one, there are two important disadvantages: 1) with very large circuits, to evaluate all the mathematical parameters, requires long computational times; 2) the dose of scanned electrons is strictly related to the developing time.

4.4 Shape Modification

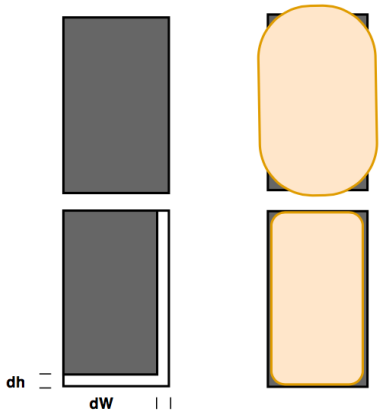

Figure 4.3: Reduction of single elements in shape modification process.

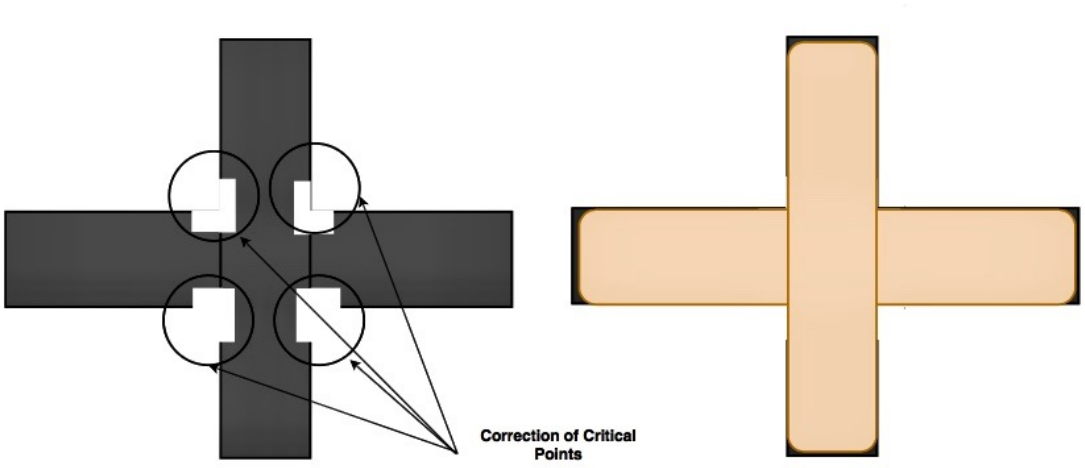

Figure 4.4: Correction of the critical points.

The shape modification process born after the development of the Dose modification method. "A well-presented method to reduce the proximity effect is PYRAMID" [40]. This method is based on the single correction of each element of the pattern thanks to the pre-calculated rule table. This rule table is evaluated from the exposure estimation. The method is divided in three following steps:

1) Reducing each rectangle size to compensate the exposure;
2) Correction of the effect related to the interaction between different parts of the circuit elements;
3) Modification of the critical-points;

4.5 Alternative PEC Method

4.5.1 Silicon Nitride/Dioxide Intermediate Layer

An alternative physical method to reduce the proximity effects is using an intermediate layer of silicon dioxide or silicon nitride before the deposition and the growth of the resist. The thickness of this intermediate layer has to be between 50 nm and 300 nm. The experiment that has shown a substantial reduction of the proximity effects was done with a particular electron beam lithography system: JEOL-JBX-5DII.
In EBL system the resolution is degraded by the scattered electrons. It is possible to minimize the number of forward scattered electrons using a thin layer of resist (no more than 100 nm) and a high level of energy beam. Nevertheless, the minimization of the back-scattered electrons results more difficult. As explained in the previous chapter, usually the material used as substrate has a large atomic number, so the number of secondary electrons produced after back-scattering phenomena is huge. Furthermore, a high value of the beam energy increases the possibility to have more back-scattered electrons because the primary ones (into the beam) can penetrate the resist deeply and easily reach the interface resist-substrate. The Monte-Carlo simulation has shown that under features of 250 nm the proximity effect starts to play an important role during the lithographic process. Using this intermediate layer could be a solution to minimize drastically this drawback that does not allow to reach a resolution of few nanometers.

4.5.2 Experiment

The experiment was done preparing firstly a Si substrate with a thickness of 400 nm. "Silicon nitride was grown by chemical vapor deposition, at 800° C on Si and at 200° C on tungsten deposited before on the Silicon substrate" [41]. The experiment was done with positive and negative resists (PMMA - SAL 601) and with and without the intermediate layer. Several thermal process conditions were developed. The resist in both cases were exposed in a JEOL JBX-5DII e-beam lithography system with an applied voltage of 50 keV and with a diameter of 15 nm. At the same time, using 8000 processors, Monte-Carlo simulations calculate the number of produced secondary electrons and their energies. The simulations took a range of 40-200 mins. All the electrons that were tracked have an energy of 500 eV. The experiment was repeated not only under different thermal conditions, but also with different thicknesses of the silicon nitride film (50 nm, 200 and 300 nm). The reason why tungesten was used also as a substrate is to analyze the reduction phenomena "on substrates of comparable atomic weight to the intermediate layer, and on substrates of higher atomic number" [41].

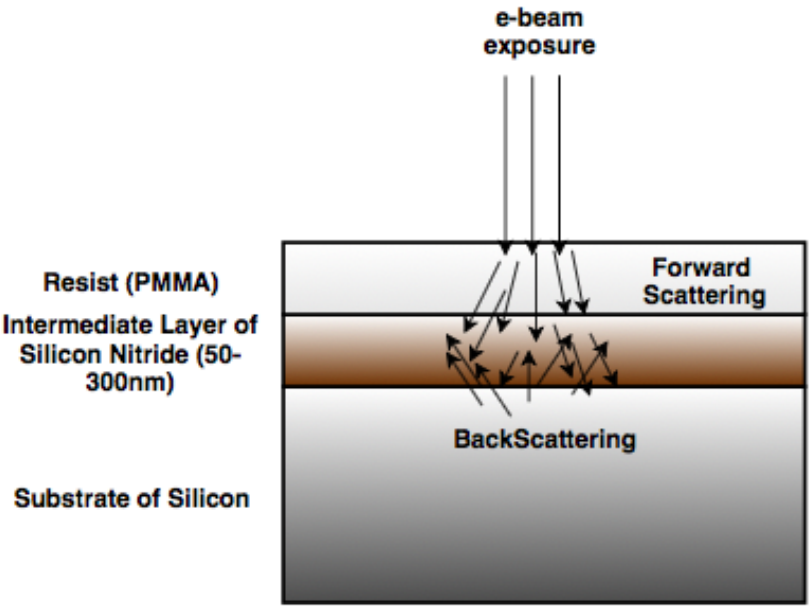

Figure 4.5: Resist, silicon nitride intermediate layer, and silicon substrate.

4.5.3 Results and Conclusion of the Experiment

The results showed that with using the intermediate layer on the Si substrate or the W substrate the number of back-scattered electrons are smaller. The reduction was observed for all the experimented thicknesses of the middle thin layer (50-200-300 nm), at different temperatures and on substrates with comparable or higher atomic weight to the middle layer. Monte Carlo simulation at the end has showed that the largest peak of the produced secondary electrons was with a film of silicon nitride of 50 nm.

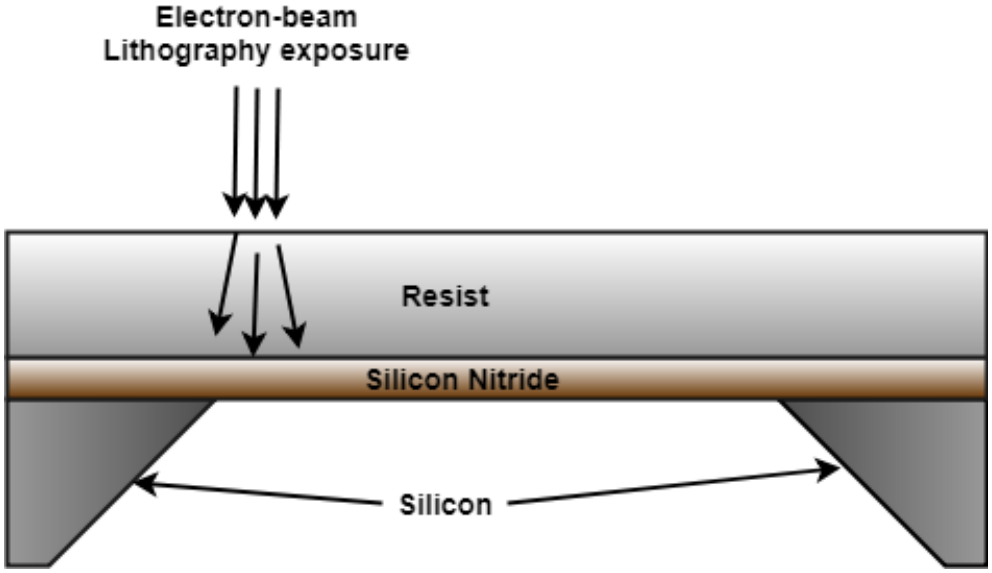

Figure 4.6: Silicon-nitrade substrate for the nano-wire of gold.

4.5.4 Membrane Structure: Silicon Nitride Substrate

As shown in Fig. 4.5 the back-scattered electrons are reduced with the use of silicon nitride as the intermediate layer, but they still provide proximity effects. If we back-etch the silicon and use silicon nitride directly as a thin substrate (as a membrane layer), it is possible to seriously eliminate the proximity effect because there wont be any interface for the secondary electrons to have collisions and generate back-scatterings. The only drawback of the silicon nitride is that it does not attach well with gold. To overcome this issue, a film layer such as Tungsten or Titanium can be used.
The process to realize a membrane structure (Fig. 4.6) will be explained in the following chapter with all the other needed fabrication processes (CVD, EBPVD, lift-off, spin coating, etc...) to obtain the single wire of Au suitable for Bis-forrecene molecules.

Chapter 5

Nanofabrication Processes for m-QCA

In this chapter the different physical fabrication processes to obtain a nano-wire of Au with a resolution of few nanometers will be described. After seeing how to avoid or reduce minimally the proximity effect with the use of the silicon nitride, analyzing the different deposition and etching processes to obtain a desired structure is needed. As mentioned in the previous chapter, before the deposition of the two metals (titanium/tungsten and gold), it is important to review how it is possible to etch the silicon substrate to obtain the same structure presented in Fig. 28.

5.1 Back-Etching Process of the Silicon

One of the reasons for the back-etching process is to generate strong membranes to support nano-structures above them. Different from Silicon, Si_3N_4 is a more adequate candidate because its strength is enough to support the entire structure. However, the silicon still remains a supporting structure for the membrane. After the chemical vapor deposition of the Silicon-Nitride, it is possible to immerse the structure in a particular solution that etches the Si from the bottom to the top until the interface Si/Si_3N_4 is reached (Wet etching). The chemical solution should not attack the Si_3N_4. The perfect candidates for this process are KOH and TMAH. The important parameters that define the quality of the etching process are manly two: the etch rate and the anisotropic/isotropic aspect of the process. The first one defines how fast the process is and usually it is measured in μ/m; the second one defines the profile of the structure and how much the etching process depends on the crystallographic orientation of the material.

5.1.1 Wet-etching

KOH is an anysotropic etchant that attacks the silicon preferably in the '100' direction and does not depend on the dopant concentration of the substrate. The etch rate is usually around 1-1.5 μm/min and it depends strongly on the composition of the solution, on the temperature of the process and the crystallographic orientation of the substrate. Usually the solution is inside a chamber that continuously is kept at 80 °C. To avoid the complete etching of the silicon substrate in '111' orientation, it is possible to use a protection layer (mask) of silicon dioxide.

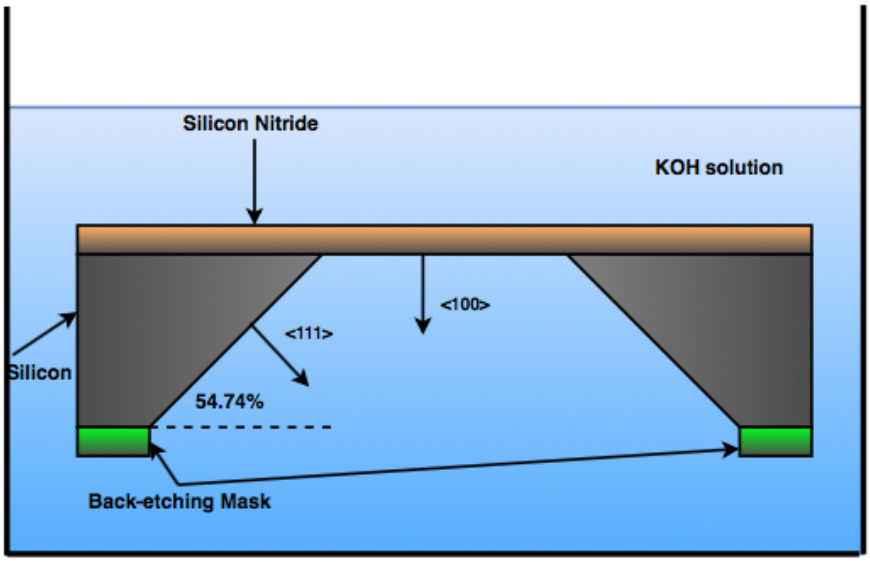

Figure 5.1: Back-etching process of silicon substrate in KOH solution.

TMAH, as KOH, is an anysotropic etchant. It was discovered more than 30 years ago and it is widely used for different MEMS applications. "TMAH is a organic hydroxide and stands for tetramethyl ammonium hydroxide" [42]. Different from the previous etchant the quantity of TMAH in the solution is around 25% and the preferred crystallographic orientation is '111'. Everything has to be kept at 95 °C. The solution does not attack silicon dioxide or silicon nitride even if they are films of few nanometers.
Another solution that could be used as an etchant for silicon is EDP. Different from TMAH and KOH, the solution is highly corrosive and very difficult to deposit. It has an etch rate of 0.02 μm/min and because of its dangerous qualities, it is not used in fab-clean room.

5.1.2 Dry-etching

For very small features, Dry-etching is used more than Wet-etching. It is a an anysotropic, non-selective process in which the exposed material is bombarded by ions and the molecules of reactive gases. It is possible to use reactive gas to etch the silicon: XeF_2. Other gases like C_4F_8, C_4F_6 can not be used because they attack normal silicon dioxide and silicon nitride. There are two kinds of dry-etching processes: Chemical dry-etching and Reactive Ion etching (RIE). The first one provides an isotropic profile with a high value of selectivity; the second one uses both physical and chemical mechanisms in order to fabricate well defined structures thanks to the directional nature of the dry etching. RIE is the most widely used etching technique because it is very fast and allows small features to generate. This last process is more expensive and more difficult to implement with respect to the wet-etching technique.

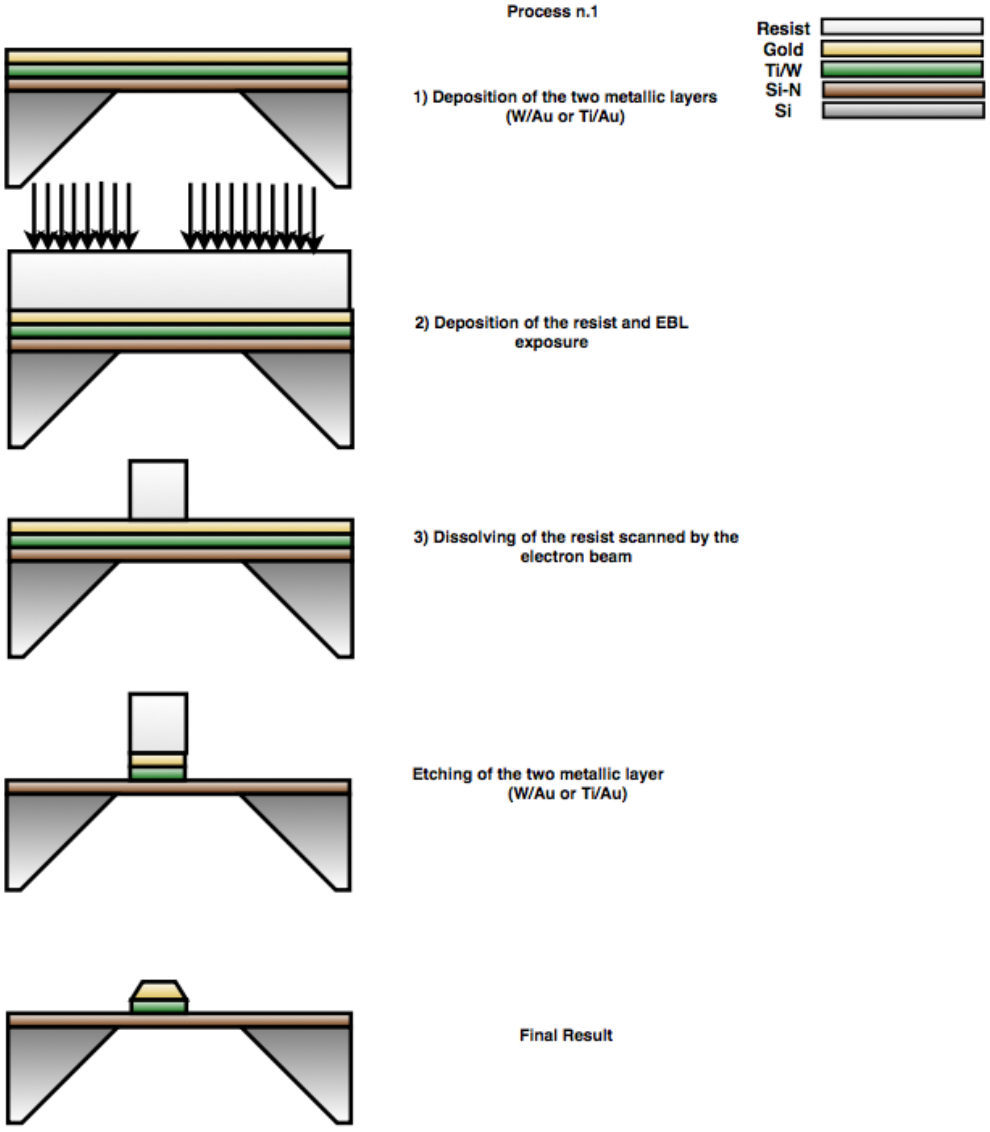

Figure 5.2: First proposed nano-fabrication process for QCA technology.

5.2 Deposition of W/Ti and Au

After the back-etching process to cut the silicon and to fabricate the membrane of silicon nitride, there are two possible way to proceed:
1) Deposition of the two metals (Ti/Au or W/Au) and of the resist, designing of the desired circuit, and under-etching to take off the parts in excess of the gold and make a structure that is thinner at the top.
2) Deposition of the resist, scanning of the pattern trough EBL, growth of the two metallic layers (Ti/Au or W/Au), lift-off process to take off the useless part.

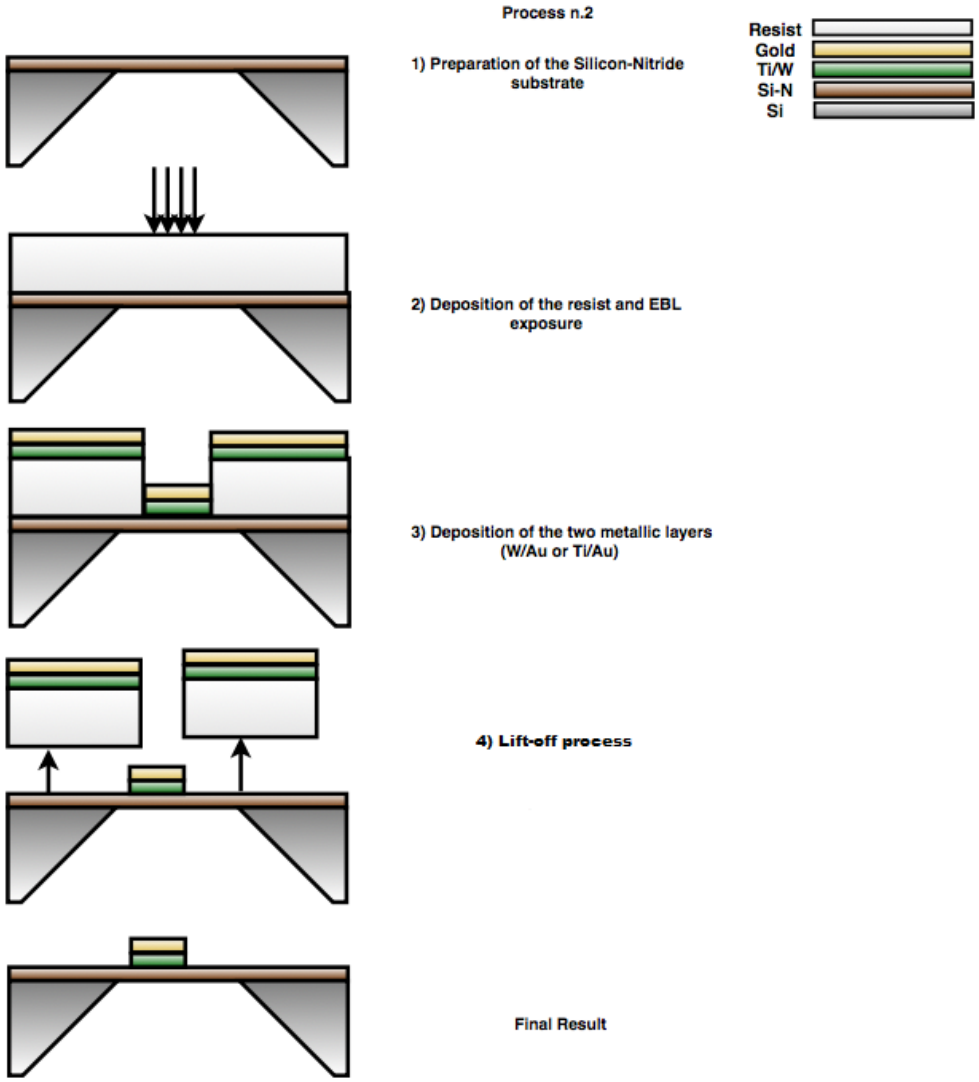

Figure 5.3: Second proposed nano-fabrication process for QCA technology.

5.2.1 Chemical Vapor Deposition

One of the most used techniques for the deposition of the metals in manufacturing and the micro-fabrication process is 'Chemical Vapor Deposition'. This technique allows the manufacturer to produce thin metallic film with high quality that can be used for high performance devices. The substrate, inside a chamber, is exposed to volatile particles of a gaseous mixture that reacts with it and the particles settle to form the layer. CVD is used for the growing of different material as metals, semiconductors (silicon, polysilicon), and insulators (silicon dioxide). For QCA-cells fabrication, the deposition of two metallic layers is important. W/Ti can be used as the intermediate layer (attaching layers) and Au as the basement for the self-assembling of the Bis-Forrecene molecules. CVD for tungsten is achieved from tungsten hexafluoride (WF_6), while for titanium it is reached thanks to tetrakis(diethylamido)titanium(IV). The two possible reactions, that release a tungsten layer, are the following ones:

$$WF_6 -> W + 3F_2 \tag{5.1}$$

$$WF_6 + 3H2 -> W + 6HF \tag{5.2}$$

The gold deposition is possible with different volatile precursors: dimethylgold(III) carboxylates, or dimethylgold(III) diethyldithiocarbamate, or CF_3Au. Nevertheless, we cannot use this technique in our case because the deposition of two different layers will break the vacuum condition and also because CVD is not used to generate very thin layers. Another technique is needed.

5.2.2 Electron Beam Physical Vapor Deposition

EBPVD is a deposition technique in which a target is bombarded with an electron gun under a vacuum condition. Derived from the electron beam melting technique, it is used for the growth of metallic and ceramic materials. The development of this fabrication process began in the early 80s and with time it has become so important for two important progresses:
1) Improvements in vacuum generation system;
2) Availability of high quality electron beam guns;

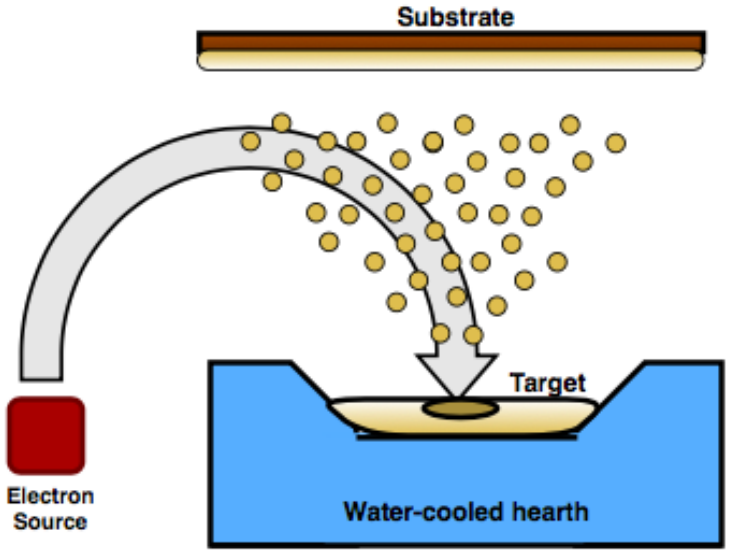

Figure 5.4: EBPVD process.

As part of the lithographic process, there are different kinds of electron sources that can be used to emit electrons. The E-beam source is placed in the bottom of the process chamber while a heated substrate is fixed at the top and it rotates on the vertical axis in order to have a homogeneous deposition of the vaporized material. To increase the kinetic energy of the electrons, a high voltage is applied (5-40 kV). The collision between the electrons of the beam and the target sublimates the material that subsequently solidifies and settles on the substrate. There are different configurations of EBPVD: one that uses a rod as target, and

another one that uses an ingot kept in a water-cooled heart. Fundamentally there are two metal evaporation methods: reactive evaporation process and co-evaporation. In the first process, the metal is evaporated by the e-beam and the volatile particles are carried by the oxygen until the reaction happens in proximity of the substrate when the thermodynamic conditions are met. The second process is used more for carbides deposition. In fact, in the chamber under vacuum there are two ingots: one of metal and one of carbide. Both are vaporized through two different electron beams and when the thermodynamic conditions are met they chemically react with each other.
"When we need to vaporize more materials and solidify them on the substrate, it is possible to use a system of multiple electron guns that work simultaneously" [43].

5.3 Resist Deposition: Spin Coating

The procedure to deposit a uniform layer on flat substrates is spin coating. This process is widely used for the deposition of resist material like PMMA. After the application of certain quantity of material in the center of the substrate, a centrifugal force rotates the substrate and spreads the coating material uniformly. The excess quantity of the coating material spins off the edge of the substrate and the process usually is stopped when the desired thickness of the resist is reached. The thickness of the resist depends strongly on the viscosity of the material. Usually the needed time to spread the coating material on the substrate is around 30-60 s.

5.4 Gold Etching Process

After the deposition of the titanium (or tungsten), and of the gold through Electron Beam Physical Vapor Deposition, the following step is the design of the desire pattern trough EBL. Because this technique is widely explained in the previous two chapters, we will continue directly to presenting how it is possible under-etching the gold below the resist to develop a structure similarly as shown in Fig. 33. gold is characterized by a high value of density 19.3 g/cm3 and as noble gases is very hard to oxidize. It requires a strong solution that is able to separate the unpaired electrons from the crystalline structure. There are different solutions that can be used to etch the gold: nitric acid and hydrochloric acid, or potassium iodide solution (KI/I_2). The first solution, better known as 'aqua ragia', is a mix between nitric acid and hydrochloric acid and works as an etchant at room temperature. The etch rate depends strongly on the temperature and it can reach 10 μm/min. The used solution can not be allowed to attack silicon or silicon nitride because they are the supporter and the substrate of the entire structure. tungsten can be attacked but, unlike gold, its etch rate is very small, and so negligible. The potassium iodide/iodine presents an etch rate of 1 µm/min, considerably smaller than aqua ragia. On the other hand, it is also possible to use reactive ion etching. The only problem of this alternative solution is the law volatility of the gold. Increasing the volatility of the gold is possible by increasing the temperature of the chamber where the etching process is developed (around 130 °C). In the case of gold the most used reaction product is $AuCl_3$. "A direct consequence of the law volatility of the gold is the easy re-deposition on the substrate inside the chamber" [44]. This provides a high value of contamination of the substrate and so subsequently a development of a cleaning wafer technique. To avoid the re-deposition of the gold, it is possible to use a thin hard mask like silicon dioxide. Another way could be electro-chemical etching, but it generates below the

resist an isotropic profile that is abnormally undercut due to the galvanic effect of the gold. This was observed multiple times in the past when the gold was attached to another metal like titanium or tungsten because together they generate a galvanic couple.

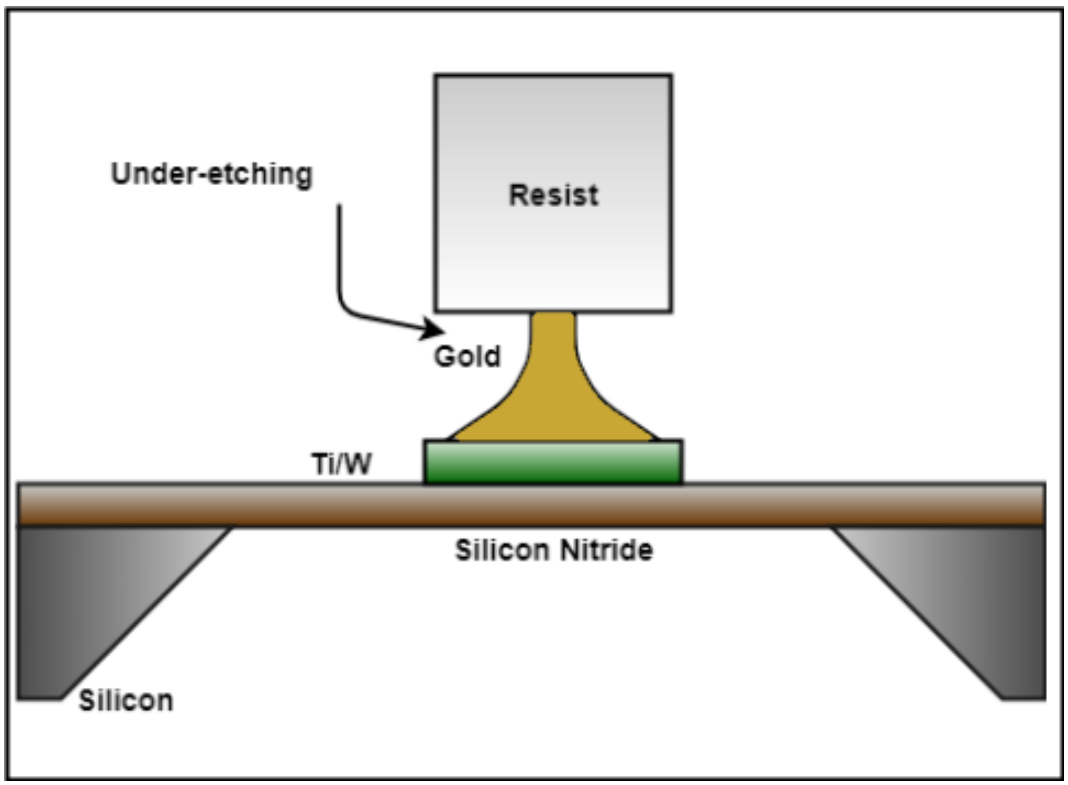

Figure 5.5: Metal deposition of titanium and gold and under-etching process.

5.5 Ti/W Etching Process

To obtain the structure in Fig. 33 a wet etching process for titanium or tungsten is needed. The wet etching process depends on which metal we used as the intermediate layer to attach the gold on silicon nitride substrate. The best candidate solution for titanium is hydrofluoric acid diluted in de-ionized water. The solution is made of 80% de-ionized water and 20% HF. Because HF attacks silicon nitride and silicon dioxide, a mask is needed to protect the parts that should not be etched. It is possible to use a photo-resist as a protection layer. The etch rate of the HF is relatively slow and it is around 0.200 μm/min. The profile of the etched material is rounded (isotropic) and selectivity is high. There are two big disadvantages to use HF in titanium etching. Taking into account the following chemical reaction:

$$Ti + 3HF- > TiF_3 + 3/2H_2 \tag{5.3}$$

it is possible to observe the titanium, reacting with HF, produces and releases H_2 that is highly flammable and explosive. Furthermore, HF is a health hazard because it can cause severe burns. To overcome some of these disadvantages it is possible to dilute together hydrofluoric acid and nitric acid.

$$Ti + 6HF + 4HNO_3- > H_2TiF_6 + 4NO_2 + 4H_20_1 \tag{5.4}$$

From the above chemical reaction it is obvious that the etching of the titanium produces hexafluorotitanic acid, nitrogen dioxide, and water. Using the mix between HF and HNO_3 the etch rate is higher and there is no generation of flammable gases anymore. Despite the increase of the etch rate, it depends strongly on the concentrations of both acids. In particular the concentrations of HNO_3 has to be four or five times higher than HF. Proportionally to the increasing of the concentration of nitric acid, the surface attack becomes uncontrollable. "The best combination of the two acids is to have an acceptable etch rate and at the same time a controllable process" [45]. If a thin layer of Tungsten is used as the intermediate layer between the gold and silicon nitride substrate, the etchant solutions will be hydrogen peroxide, sodium nitride diluted in water, or also the simple mix $HF - HNO_3$. The first two solutions have a very high etch rate, so normally they are used for structures of few μm. The deposited films for a physical implementation of mQCA technology are very thin,so the etch rate of the etching solution should not be very high. As mentioned before in the case of $HF - HNO_3$, the composition of the two acids is very important to define how rapidly the solution will attack the film. Considering that the intermediate layer of tungsten is very thin, to have a controllable process the best ratio between the two acids (HF and HNO_3 respectively) has to be 1:2.

5.6 Lift-off Technique

Lift-off process is a fabrication process that, opposite to the normal subtracting techniques like etching, allows to generate micro or nano structures using sacrificial material (resists). This technique is widely used when a direct etching of the material is not possible considering the undesirable effects that could affect the layer below. Furthermore, with respect to the etching process, it is cheaper and easier to implement. In our presented structure, only the material that is directly attached to the substrate in the hole will stay. The other part of the material will be washed out with the resist layer. Everything happens with the structure immersed in a solution that is capable to dissolve the resist.
An important parameter that defines the effective possibility to implement this technique is the ratio between the resist and the layers above. This ration has to be at least 10 or greater. The biggest disadvantages of this fabrication process are: retention, formation of undesired projections and redeposition.

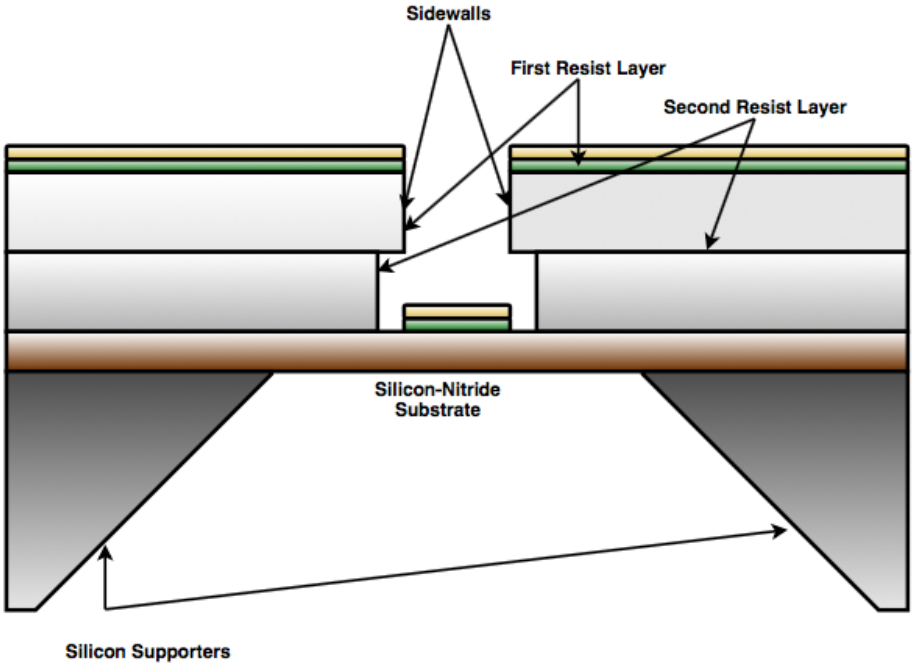

Figure 5.6: Double layer of resists to overcome the extra-deposition on the sidewalls of the metal.

The first problem is related to the unwanted part of the metal that remains after the washing process. This happens especially when the resist does not dissolve well. The second problem is related to the deposition of the metals inside the holes. Part of the material deposits on the sidewall of the holes and will remain also after the lift-off process. The last problem depends on the volatility of the metals, because it could happen that some particles will become reattached to the surface. Despite these negative aspects, since the process is very easy to implement, it is widely used in micro and nano fabrication. It requests at maximum wet bench and ultrasonic agitation. Overcoming the formation of the projections on the sidewalls of the features designed into the resist layer is possible with different methods. One is a technique that has been used to generate re-entrant profiles of the resist as shown in Fig. 5.7. This treatment (Soak process) can be done by overexposing the resist in a solution environment (chlorobenzene, toluene, bromobenzene, kerosene, or fluorobenzene) and by baking at a high temperature (80 °C-100 °C). Another possibility would be to deposit two layers of resists. They should have two different viscosity coefficients such as DQN and PMMA. After the deposition of PMMA, the second layer of the resist on the top will be spun, exposed, and then developed. This process is too complex to implement. Due to the difficulty of this technique, the most common method to avoid deposition on the sidewall of the features remain the one firstly proposed. "The soak process can be done by using as compound fluorebenzene which reduces the the dissolution rate of the resist at the surface" [46]. The thickness of the ledges depends on the time of the process and the temperature.

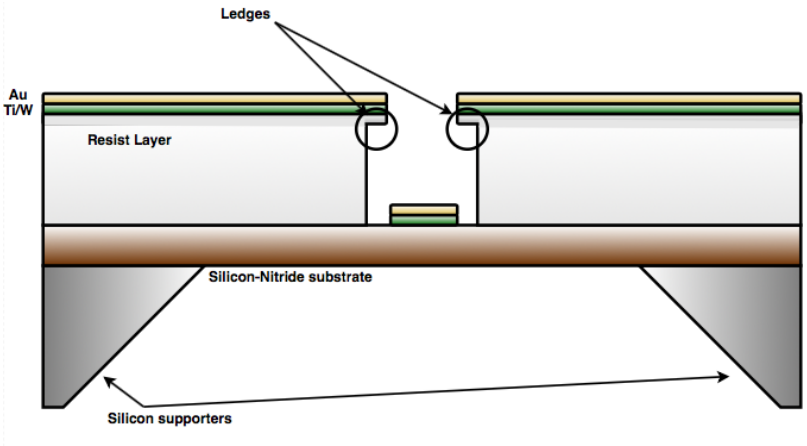

Figure 5.7: Soak process as solution for metal deposition on the sidewalls of the resist.

Chapter 6

Electron Microscopy

6.1 Testing: Ultra-microscopy

Verifying a fabricated nano-structure in the lab is the last but not the least step of the process. After the different considerations and explanations about the different nano-fabrication processes to provide a suitable structure for QCA technology, a short description of high resolution microscopy is significant. Particularly, the most widely used electron microscopes are: TEM and SEM. They are used to analyze the structure, composition, and properties of the sample in nano details. The different functionalities of a TEM/SEM like imaging of the morphology of the sample, constructing a 3-dimensional image, viewing frozen material,and generating x-rays for microanalysis, have made these kinds of microscopes significant for various application fields (material science, geology, environmental science, nanotechnology and electronic).

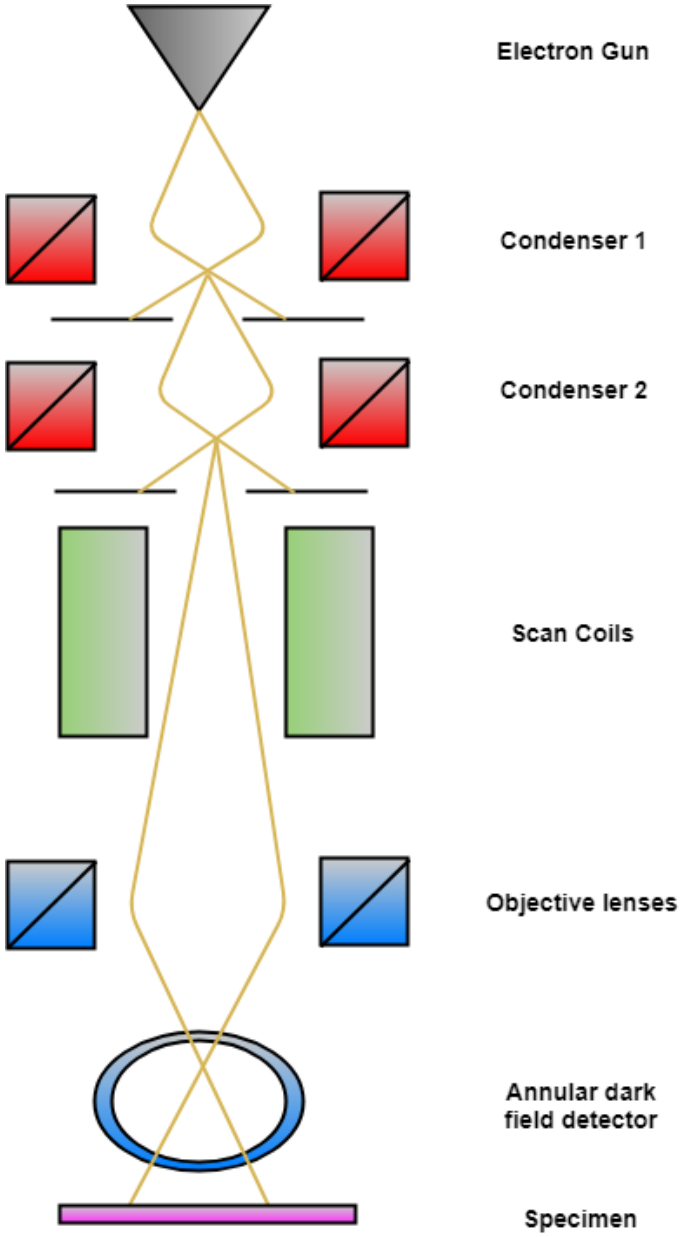

Figure 6.1: SEM system structure.

6.2 SEM: Scanning Electron Microscopy

The Scanning Electron Microscopy is an imaging technique that used an electron beam instead of the normal light. The primary electrons that made the beam scan a sample point by point. The interactions between the atoms of the sample and the primary electrons generates other particles: electrons (secondary), back-scattered electrons, x-rays that are revealed and then transferred as electric pulses to a image system (monitor). The result of this process is typically an image with a high resolution (5-1 nm). As any electron system, everything must be kept under vacuum condition because the presence of the air and the resulting collisions with the primary electrons could affect the resolution of the process. The sample should be

prepared before to be subjected to the electron beam under vacuum condition. It is usually mounted rigidly on a holder that is a bit larger, and it is made of material with a significant electrical conductivity like gold, platinum, or tungsten.
As in EBL and TEM, the electrons are extrapolated from a source (filament of tungsten or LaB_6) and directed towards the sample. The electron beam has an energy around 30 kV and it is led through a system of deflectors, apertures and lenses. In particular the lenses and the apertures are needed to focus the beam and pull out the electrons that are far from the central axis of the SEM column, while the deflector deflects the beam to obtain the required scansion. When the electrons collide with the atoms of the sample, they lose energy and they generate scatterings. The material of the specimen is significant because the clarity of the image depends on it. Usually a sample with a high atomic number (Z) generates a darker and more visible image; while a specimen with a low atomic number, provides an image that is less dark and not well defined.
After the collisions, a computer monitor with a proper amplifier system is used to reproduce the distribution map of the intensity of the signal scanned over the sample. If it is necessary the image is also magnified. The magnification system can operate in range of magnification between 10 to 500. Nevertheless the several improvements, the limitation of the resolution represents the major drawback of this microscope. Unlike the optical microscope, the resolution is not limited by the wavelength of the used irradiation, but by the interaction volume and the thickness of the specimen. Unfortunately, very high resolutions (enough to detect atoms or molecules) are not reachable. A different microscopy system is needed.

6.3 TEM: Transmission Electron Microscopy

Demonstrated by Max Knoll and Ernst Ruska in 1931 for the first time [47], Transmission Electron Microscopy is one of the widest used imaging techniques to capture images of very small things like single atoms or molecules. It is a distinguishable process from the normal light microscopes because it is able to image at a very high resolution, owing to the wavelength of the electrons. For this reason it finds application in material sciences, virology, medicine, semiconductor studies, and nanotechnology research. As the name announced, an electron beam is transmitted over a specimen on which the image is reproduced. The generation of the image is possible thanks to the interaction between the electrons of the beam and the sample. The focusing and magnification of the image are provided by an imaging device, usually a photographic layer or a fluorescent film. As explained before for EBL systems, a transmission electron microscope consists of different components.

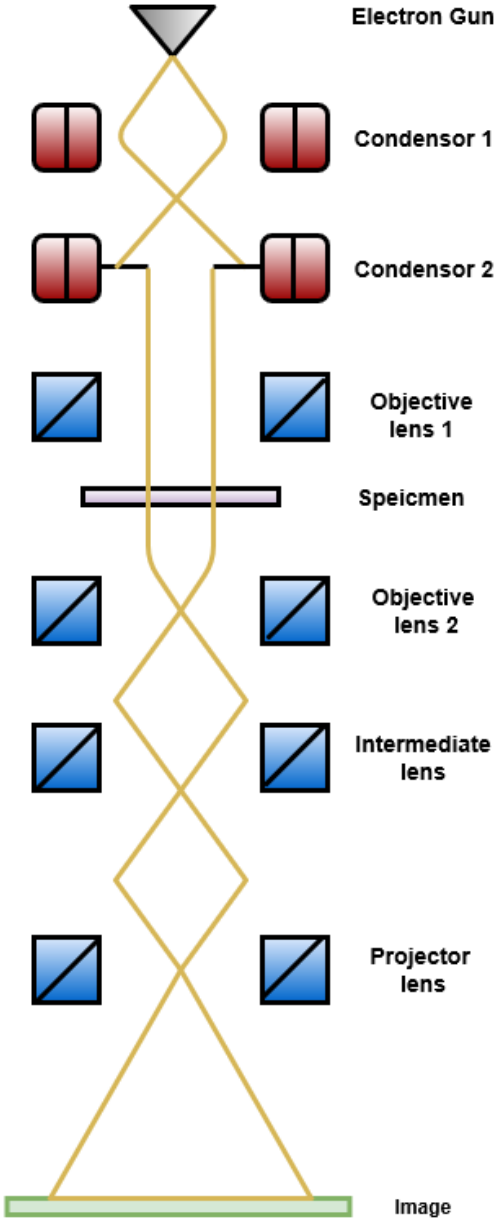

Figure 6.2: TEM system components.

A vacuum system for a standard TEM is generally evacuated to low pressures (10^{-5} Pa). These pressures are achieved thanks to a rotary vane pump, a system developed in 1874 by Charles C. Barnes and widely used for vacuum experiments in physics. Keeping the vacuum conditions is essential because the collisions between electrons and gas atoms/molecules must be negligible. However, there are some components like the specimen holders and film cartridges that have to be periodically inserted, causing losses in vacuum condition.
The specimen system consists of different components like airlocks, holders, a grid, and a stepper motor controlled by a trackball. The airlocks allow the insertion of the specimen inside the chamber without breaking the vacuum condition, or minimizing the losses. The holder is usually a supporter for the grid with a size of 3 mm and a thickness of 100 μm. There are several holders and their use depends on which kind of experiment is performed.

The grid is positioned above the holder and is usually 0.5 mm smaller than its supporters. It can be made of different materials like copper, platinum, or gold. Inside the chamber, to relocate the specimen in the region that are interested by the electron beam, a TEM stage is used. Usually, especially in the newest versions of this kind of electron microscope, electrical stages are used. They consist in a stepper motor that moves the sample under the beam, and a controller that decide the following movements like a trackball.
The electron gun is the same system that is used inside the electron beam lithography. It consists of an electron source (usually a filament of tungsten), a biasing circuit, a Wehnelt cup (cathode), and an extractor (anode). The electrons are extracted from the filament and pulled towards the anode where there is a hole that represents the beginning of the TEM column. As mentioned in the third chapter there are different electron sources. Because the amount of electrons depends on the work function of the material of the filament, the choice of it is important. Furthermore, in order to achieve a thermionic emission it is important to heat the source.
The electric-magnetic lenses are needed to focus the beam. Usually these lenses are convex, coated by an electromagnetic material like iron, nickel, or cobalt [48]. The choice of the coating material depends on its magnetic parameters like hysteresis, magnetization, and permeability.
The apertures, as in a EBL system are used to pull out the electrons that are too far from the optic axis. They are characterized by metallic plates that are thick enough to filter the electrons. The use of the apertures causes two important drawbacks: the scattering of the electrons that can create aberration phenomena, and the reducing of the beam in terms of intensity. However, the reachable resolution with these microscopes is around 0.1 nm, which is high enough to obtain a detailed image of atoms and molecules. The image is collected thanks to a viewing screen and a binocular that focuses the image. A CCD camera is inserted inside the path of the beam in order to collect the image in a digital form. An updated version of a trasmission electron microscope is STEM (Scanning Transmission Electron microscope). Different from the first one, STEM uses an annular dark detector for the formation of the image. The image forms thanks to the forward-scattered electrons that collide on the annular detector. By using an ADF detector it is possible to reach incredible resolution and provide atomic images [50]. In the following sections the aberration phenomenon that limits the resolution of the electron microscopes and the improvements provided in the last 30 years will be addressed.

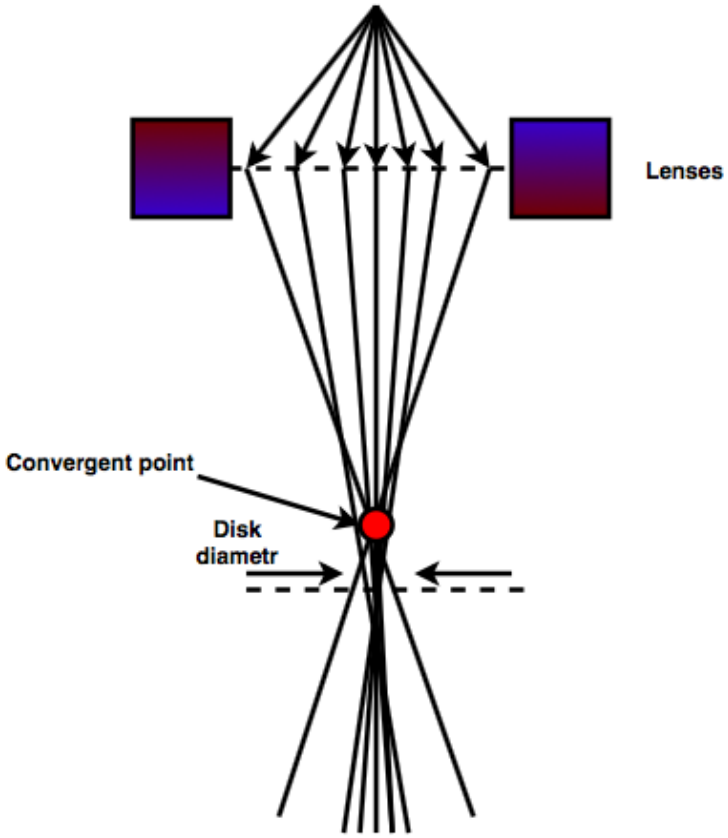

Figure 6.3: Spherical aberration.

6.4 Aberration

One of the most important factors that limit the resolution of TE-microscopes is the quality of the objective lenses. Usually, the use of in-homogeneously lenses cause a phenomenon that is called spherical aberration. Practically, the rays that are parallel to the optic axis and hit the lenses should converge in at the same point. Instead of a convergence of a one point, the final result consists of an imaged disk with a certain diameter. From the equation 3.10, it is possible to notice that the diameter of the disk depends on the aperture of the electron beam and on the spherical aberration coefficient C_S. The chromatic aberration, different from the spherical ones, depends on the amount of energy that the electrons lose when they pass through the lenses. The electrons, that come out from the gun, are characterized by the same level of energy. When they are bent from the objective lenses, they lose energy and, as for spherical aberration a disk image is generated. The diameter of it (see eq. 3.11) depends on the chromatic coefficient, on the applied voltage to accelerate the electrons, and on the lost energy of each electron.

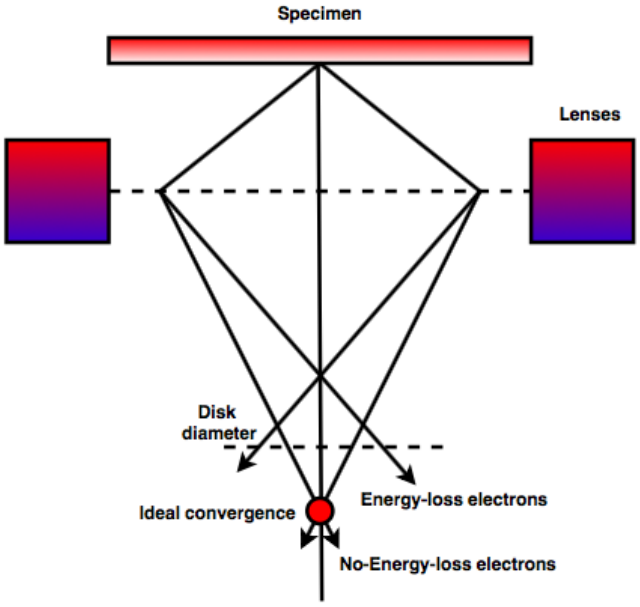

Figure 6.4: Chromatic aberration.

Another important phenomenon that could happen when the beam is not exposed at uniform magnetic field is astigmatism. The non uniform magnetic field changes the circular shape of the beam into an elliptical one. This problem is related to the fabrication inside the lenses of the iron pole pieces that should be equal. As explained for EBL systems, the astigmatism can be corrected by using the stigmators. Sometimes it can happen that the electron beam of a microscope is off-axial or oblique in respect to the optical axis. This phenomenon is known as coma aberration and it can be overcome by involving proper adjustment of the beam.

6.4.1 Background of Aberration Corrector

The fact that the aberration phenomena represents an issue for high-resolution microscopy has been known since 1936. The first idea to overcome this problem was proposed in 1947 by Scherzer. He thought an aberration corrector consisted of cylindrical lenses, replaced then with quadrupoles and octopoles. In 1961 it was showed that the insertion of a mix of quadropoles could minimize the effects of chromaatic and spherical aberration. In 1990, the EMBL (European Molecular Biology Laboratory) made an attempt to correct the aberrations and the results were astonishing. "By using a quadropole system of lenses, the resolution of the instrument went from 5 nm to 1 nm" [49]. After that improvement, a sextupole system was proposed to replace the quadrupole. In 1995, it was shown that it works better inside a 200 kV TEM with a LaB_6 electron source. The next stage was to install the aberration correctors inside the newest electron microscopes characterized by the Schottky-emission gun. Mounting a sextupole system on Schottky-emission TEM showed a significant increasing of the resolution that reached almost 0.24 nm. The sextupole corrector that was presented by Haider, reached a resolution of 1.4 angstroms and the results, after different rejections, were published in 1998. The following step was to correct the aberrations, but at same time limiting the probe size of the Vacuum Generator implemented in TEMs. This was possible by mixing the quadropole and octupole correctors. At the end of the 90's the proposed systems

to correct the aberrations were principally two: CEOS corrector (Heider and Zach) and NIOS corrector (Krivanek and Delby). In 1997, placing a NIOS corrector into a VG HB501 STEM system an effective reduction of the probe size of the Vacuum Generator was showed. Consisting of a combination of quadrupoles and octupoles, the system reached a resolution of 1.24 angstroms. On the other hand, Haider and Zach developed a corrector that consisted of only sextupole systems.
Neverthless, even though the improvements and adjustments for both correctors had been developed, finding a way to correct the other kinds of aberrations (third-order geometrical aberration, fifth-order geometrical aberrations, parasitic aberration, and anysotropic and isotropic coma) was still needed. To overcome all this phenomena that affects the resolution in a microscopy system, some adjustment and improvements were needed. These were provided by Rose in 2000 when he presented the Superplanator that consisted of two quintiplets of quadrupole and three octupoles. Unfortunately this corrector did not show the wanted results and was replaces by Ultracorrector. It was made of two similar parts (symmetric and asymmetric), each one consisted of a sequence of seven quadrupoles and seven octupoles. The development of this corrector allowed the correction of the third-order and fifth-order geometrical aberrations, but not the chromatic one. To overcome this problem, in 2002 Zach and Heider included inside their SEM, characterized by a sextupole system, a mix of electro-magnetic quadrupoles. Because mounting the electro-magnetic quadrupoles in a SEM system made of sextupole correctors is too difficult, manufacturers today prefer other methods: for example limiting the energy spread of the beam. In 2004 the FEI Tecnai F20ST trasmission electron microscope was presented by Freitag. It consisted of a monochromator to correct the chromatic aberration and an appropriate system of CEOS sextupole corrector. The reached resolution with this microscope was around 1 angstrom. The following notable stage was in 2009 when an improved version of the JEO TEM, developed at Oxford University (2004), reached a resolution of about 47 pm. In 2010 Krivanek presented Gentle STEM. It operated at a voltage of 60 kV and provided a resolution high enough to describe structures atom-by-atom. It was a result that since that time no one had reached.

6.5 Imaging Theory in Electron Microscopy

The wavelength of the electrons, as in EBL system, depends principally on the accelerating voltage as illustrated in the following equation:

$$\lambda = \frac{h}{\sqrt{2 * m * e * V}} \tag{6.1}$$

where m the electron mass, e the electronic charge, V the applied voltage, and h the Planck's constant. The higher the applied voltage to accelerate the electrons is, the smaller the wavelength will be and the higher the achievable resolution. There are different kinds of images that can be produced by the microscope. One of them being the bright field image. The areas that absorb the electrons appear darker while the regions that transmit the electrons appear brighter. To simplify, the image is the 'shadow' of the specimen. To increase or decrease the contrast of the image, objective aperture are implemented to select the unscattered electrons.
Dark field images, different from the bright field image, use the secondary electrons (or scattered) to form the image. The areas where the scatterings do not occurs appear dark. Usually this technique is widely used for analyzing the crystalline structure of the materials and their defects.

In the Diffraction mode the image is formed thanks to the scattering phenomena that occurs when the electron beam passes through a crystalline sample (specimen). The final result will be an image characterized by a series of dots. This imaging mode is widely used to characterize the crystal structure of the material. In the transmission electron microscope the images are formed in two different steps. As showed in Fig. 6.3, the primary image is formed when the electrons are scattered and pass through the specimen and the beam is focused thanks to the objective lenses. They formed a diffraction pattern which represents "the Fourier transform of the scattered electron wave" [51]. "The primary image is the Anti-Fourier transform of the diffraction pattern" [51]. After that, additional lenses are used to magnify and produced the final image. Before explaining how the images in microscope are formed, it is fundamental to define some important quantities that are essential to understand the imaging theory in microscopy. The are three different planes:

1) the objective plane contains the object point and is always above the lens;
2) the image plane that is always below the lens and consists of image points;
3) the focal plane of the lens where the parallel rays cross each other and are brought to focus.

As "distances" there are:

1) the objective distance from the specimen to the objective lens;
2) the image distance from the final lens to the image plane;
3) the focal distance from the lens to the focal plane;
4) the camera distance from the sample to the final image that depends strongly on the lens system.

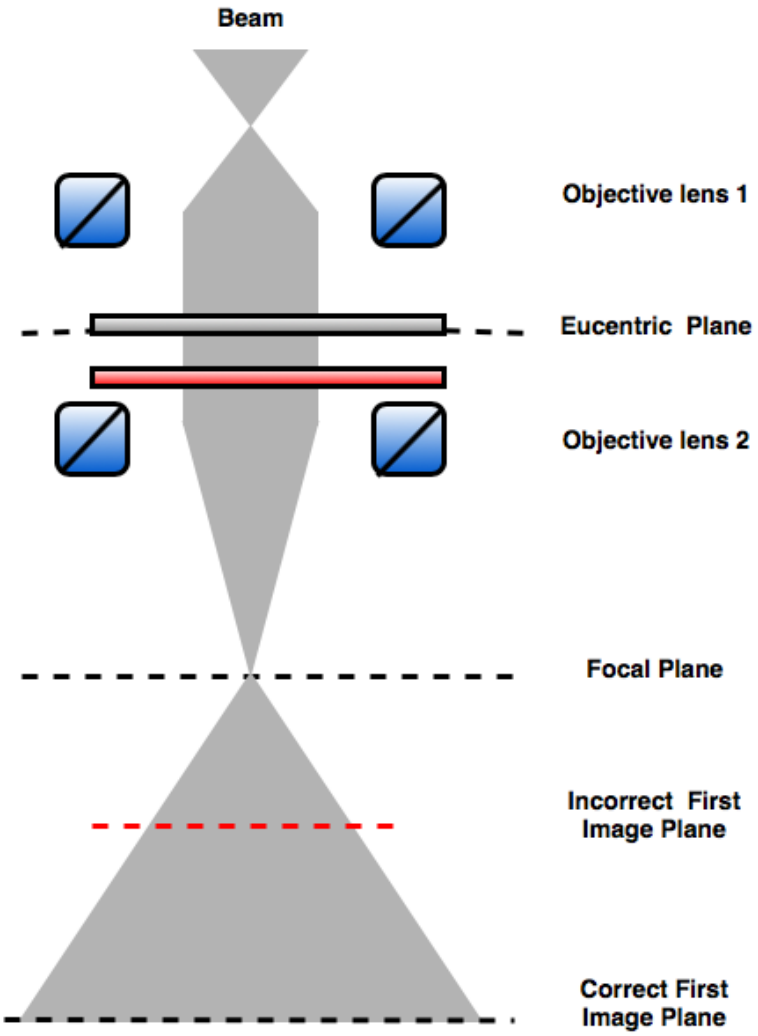

Figure 6.5: Diffraction and Eucentric plane.

The sample that scans the electrons works as a diffraction grid: some electrons pass through and others are scattered out. The contrast that defines the image of the sample depends strongly on the scattering phenomena and its nature. In the DFI (Dark Field Image) mode, some regions can appear darker due to fewer electrons that cross the sample, or because some regions of the sample are thicker than the others. The diffraction phenomena depends on the crystalline structure of the sample. The distance between the direction of the unscattered electrons, and the direction of the scattered electrons, is inversely proportional to the corresponding lattice spacing in the specimen. The higher space between the atoms in the sample, the higher the wavelength of the primary electrons will be. The position of the sample between the first and second objective lenses is important to define the image distance. It has to be located in a plane that is called the 'Eucentric' plane.
The appearance of the diffraction pattern depends on the position of the specimen in the x-y plane, considering that the z-axis is the optical axis of the beam and is perpendicular to the image plane. In order to satisfy the Bragg condition, the specimen is tilted in the three directions with two holders: single-tilt and double-tilt. The single one moves the specimen on the

z-axis to center the sample at the 'Eucentric' plane, and the double one moves it on the x-y plane. The sample is oriented to achieve a distinctive diffraction pattern. Below the objective lenses, a system of multiple lenses (intermediate and projection) allows the magnification of the primary image and provides the final image collected by the detector.

6.6 Environmental Microscope

TEM, as explained before, provides very high resolution images of thin specimens. However, the applicability is limited due to the requirement of a high internal vacuum. The high vacuum condition precludes at these microscopes, the study of living specimens, or specimens in gas or liquid environments. Nowadays, to overcome this problem, E-TEM (Environmental Transmission Electron Microscope) has proposed and has received increasing attention, especially from material scientists. This kind of microscope can operate out of the vacuum condition. The first idea to fabricate it was to introduce an E-cell inside a normal TEM confined by electron transparent windows. The material of the windows is amorphous silica, or carbon, in order to minimize the diffraction phenomena inside the chamber with the primary electrons. The advantages of the E-cell are the low cost and the low invasiveness because it is not necessary to change anything inside the microscope. The disadvantages are that the total thickness of the cell, and the presence of a gas or of a liquid, make the resolution of the collected images worse. Heating the specimen or applying a high voltage can not be considered solutions because both actions would damage the sample and the windows.
The second proposed idea was to introduce a specific differential pumping system inside the microscope that, like a system of multi-compartments, pumps out the gas in two different steps. "This assures no significant changes in the TEM column vacuum occurs when the gas enters inside the specimen area" [52]. The most important advantage is that the sample is directly exposed to the beam. In this way, the resolution does not decrease. The disadvantage is the introduction of the differential pump, which is complicated because it requires a long time for installation. Furthermore, the cost of the machine doubles. Despite these challenges, the highest achievable resolution is around 1 nm. With the increased interest in nanotechnology, and thanks to the reachable resolution, in the future the demand of this new microscope will increase rapidly.

Chapter 7

Results of Nanowire Fabrication Processes

In this chapter some results of previous experiments will be addressed highlighting the highest resolution reached in the Nanotechnology Core Facility of UIC (NCF) and the challenges for the fabrication a very small features.

7.1 Nanotechnology Core Facility at UIC

The Nanotechnology Core Facility (NCF), located in the Engineering Research Facility (ERF) is a well equipped clean-room located at Univeristy of Illinois at Chicago. It provides many nano and micro-machines used for studies and researches. Inside the clean-room is possible to design integrated circuit and to develop MEMS and NEMS applications, and nano devices.

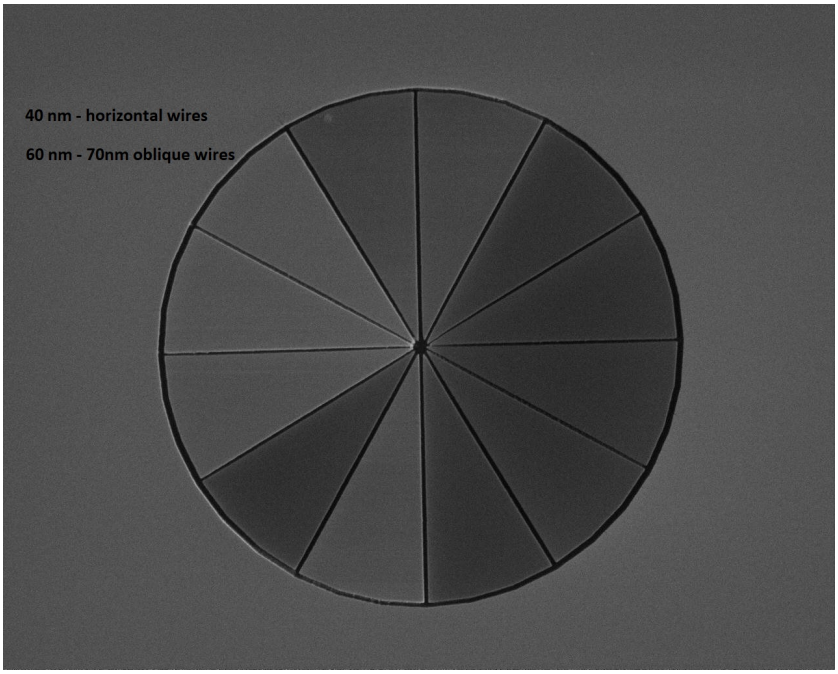

Figure 7.1: Depending of the nanowires on the orientation on the fabrication plane.

7.2 Resolution of the Developed Nano-wires

The E-beam lithographic machine used inside the clean-room to produce the pattern for nanowires (Fig. 7.1-7.2-7.3) is Raith-100. The Results, detected through a scanning electron microscope, showed that the thickness of the different wires depends strongly on their orientation. The horizontal and the vertical wires are less wide then the oblique ones. Some directions are more sensible to the micro vibrations that can occur during the fabrication processes. To overcome this problem, the NCF has bought a new microvibration isolation system that cost more than 100k dollars to guarantee stability and isolate the equipment from any kind of vibration. In the Fig. 7.2 and 7.3 the intersection between two or more nanowires are shown. As it is possible to see from the pictures, the proximity effect is well visible in the critical point (intersection between nanowires), where the dimension of both wires increase generating a no perfect cross.

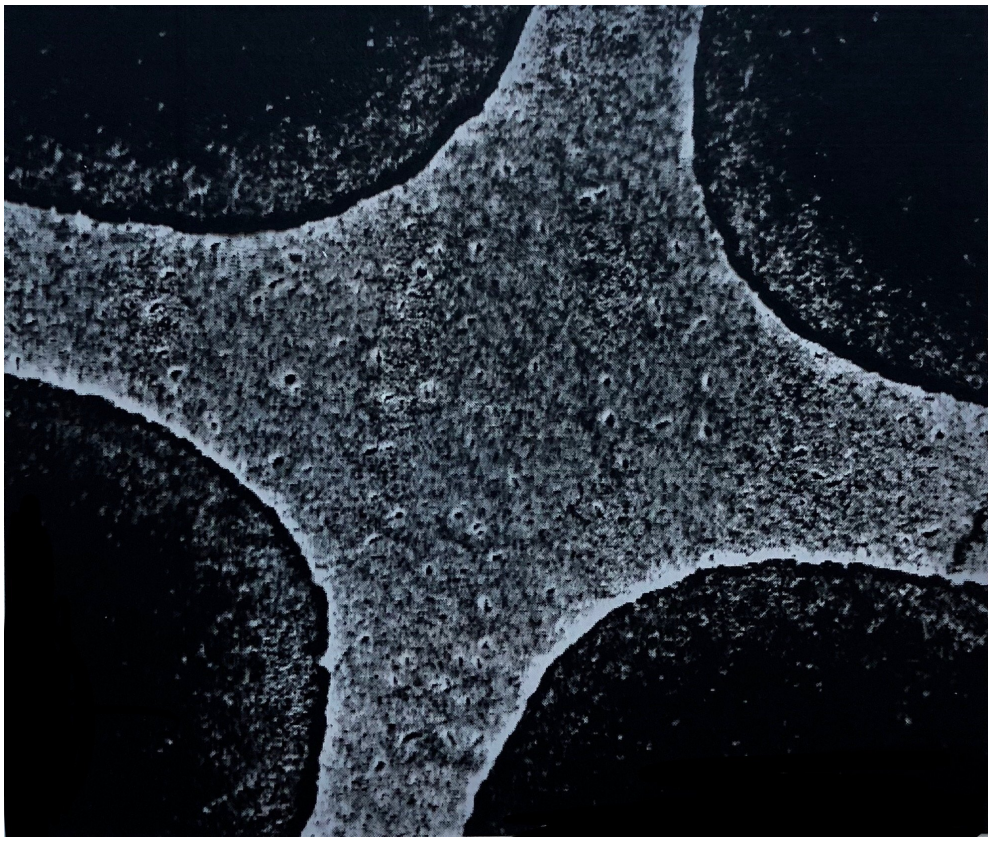

Figure 7.2: Proximity effect at the intersection point between two nanowires.

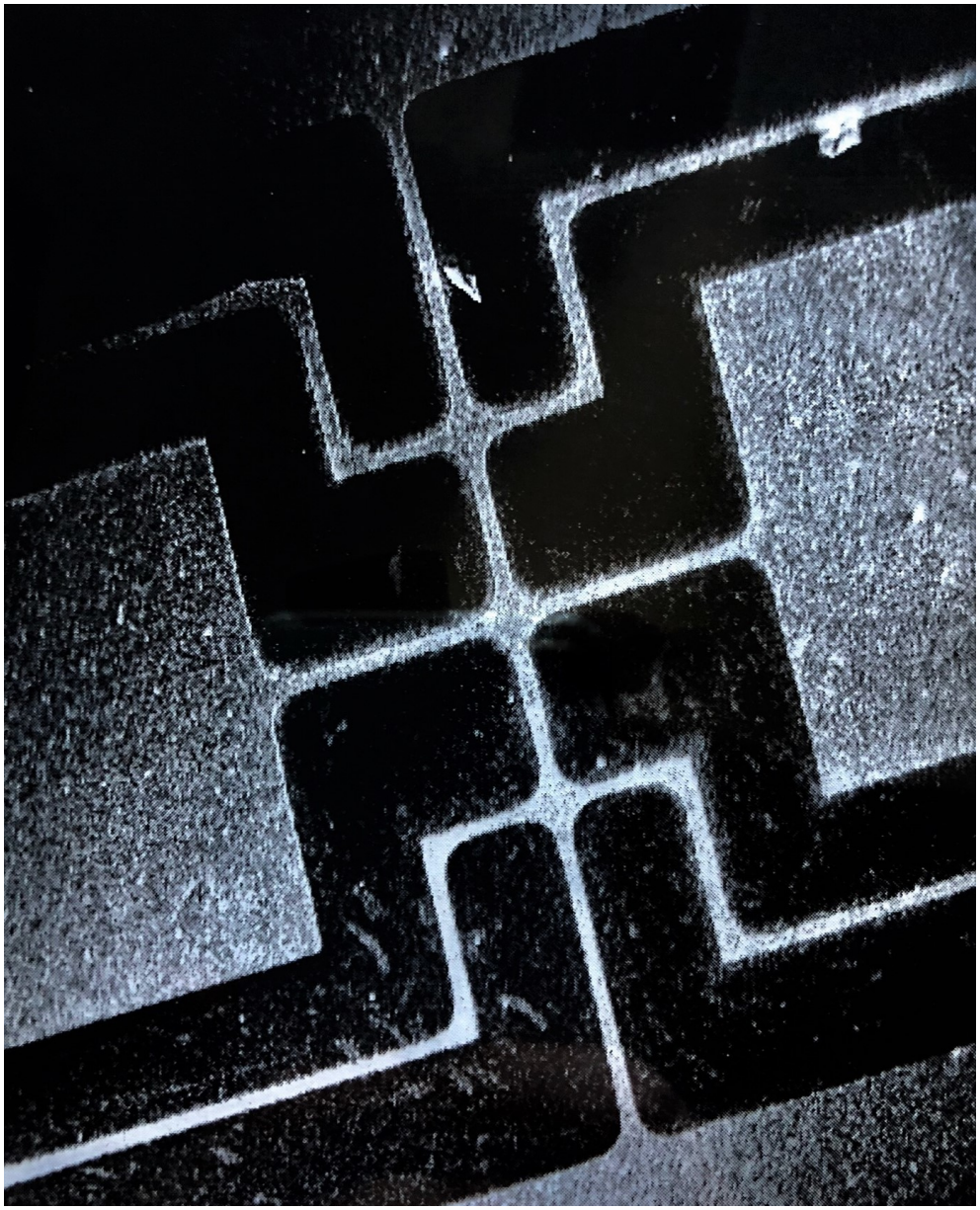

Figure 7.3: Nanowires with a resolution of 40/50 nm.

The reachable resolution of the horizontal single wire is 40-50 nm by using the mentioned EBL system. Despite the precision of this technique, the resolution is not high enough to produce a nanowire for a single alignments of the molecules. Because of the spontaneous attaching of the molecules, the single wire must respect the dimension of the molecules (not wider than 2.5-3 nm). A wider wire means a misalignment of the molecules and so a not successful propagation of the information between the neighborhood molecules. Unfortunately to handle these small molecules (Bis-Forrecene) is not easy and it requires sub-nanoscale equipment. This is the biggest issue of this new storage and logic technology and the reason why everything for now represents still remains only a theoretical idea.

Chapter 8

Conclusion

The work of this master thesis focuses on the characterization of the different fabrication processes to implement physically one of the most promising storage technologies. As described in the introduction, a prototype of molecules was presented by Polytechnic of Turin. Different simulations in Matlab and Comsol were done by my colleagues Doffo and Polsinelli in their master thesis to prove that the proposed and studied technology works. Nevertheless, the biggest limitation remains the low resolution of the processes. The dimensions of the molecules are very small (nm or sub-nm) and assembling them on the nanowire inside a binding structure is very difficult. It was also thought to generate more alignments on a single wider wire but, because the molecules spontaneously attach to the surface without a precise order, as the technology requires, that idea is impossible to implement. Identifying and describing all the problems that occur during the realization of the QCA device was the aim of this work. In the near future, when the equipment inside the clean-rooms will be more precise and the resolution will be high enough, the production of the molecular QCA devices will be fully realized.

8.1 Future Plan

Organic QCA represents an optimal solutions to replace CMOS technology for the electronic world. After describing all the nano-fabrication processes, the challenges, and the physical limits of this technology, the next step of this work will be to submit a proposal to Argonne National Laboratory here in Chicago. The company provides a better EBL system and more advanced machines than the ones provided by Nanotech Core Faciity at UIC. In the mean time, here at UIC, it is possible to follow an unusual process to fabricate crosses of nanowires that are fundamental for the physical implementation of Organic QCA technology. This unusual process let us to turn the 'disadvantages' of an EBL system in 'advantages' and reach a better resolution. The idea of this technique is to use an EBL system to pattern different fields. In order to obtain a perfect field without distortion, the minimum size should be not less than 50 nm per side. The total pattern will be divided so in different fields and they will be designed step by step, one by one as shown in the fig. 8.1.

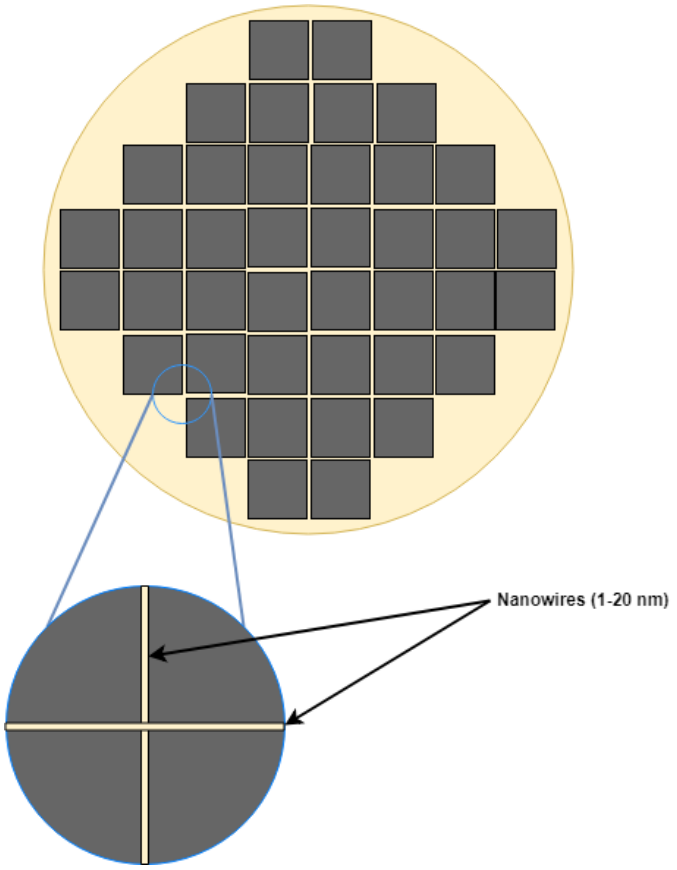

Figure 8.1: Substrate with different fields

When more fields are patterned, there is an error called 'stitching error'. It forms spaces between the different fields due to the optical imperfections of the EBL system.

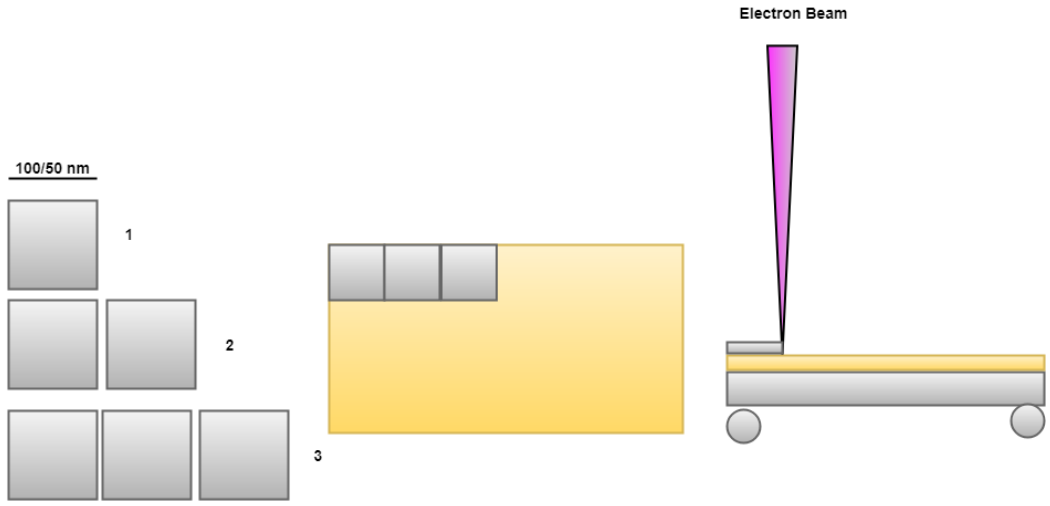

Figure 8.2: Fabrication of different fields of 100/50 nm per side

If we look carefully the structure that comes out, the different spaces are nothing more than nanowires that, crossing each other, generate a grid structure. The stitching error is

not predictable but the resolution of the generated features is very high. It could be between 1-20 nm. Because for this technique any kind of substrate can be used, after the designing of the various fields on gold substrate, it is possible to self-assemble the molecules and check which nanowire is good enough. As mentioned before, the results of this process can not be predicted, but it's an alternative way that allow us to fabricate features with higher resolution.

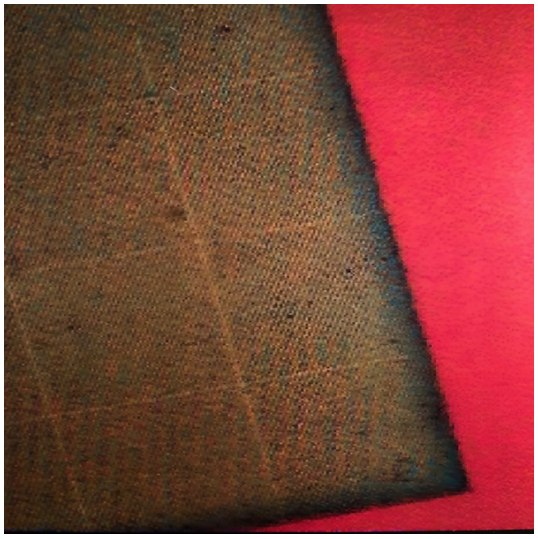

Figure 8.3: Visible spaces between different fields due to the stitching error (SEM image).

List of Figures

List of Tables

Bibliography

[1] Bhushan, Bharat: *Encyclopedia of nanotechnology*, 544.1 ENC, Springer The Netherlands, 2012. 1

[2] Beckett, Paul and Jennings, Andrew: *Towards nanocomputer architecture*,Australian Computer Science Communications, vol. 24, n. 3, pag. 141-150, 2002, IEEE Computer Society Press. 1, 2

[3] Amiri, Mohammad Amin and Mahdavi, Mojdeh and Mirzakuchaki, Sattar: *QCA implementation of a mux-based FPGA CLB*, Nanoscience and Nanotechnology, ICONN 2008, pag. 141-144, 2008, IEEE. 1

[4] Sui, Bing-cai and Chi, Ya-qing and Zhou, Hai-liang and Xing, Zuo-cheng and Fang, Liang: *Reconfigurable single-electron transistor logic gates*, Solid-State and Integrated-Circuit Technology, 2008, ICSICT 2008, 9th International Conference on, pag. 567-570, IEEE. 4

[5] Niamat, Mohammed and Panuganti, Sowmya and Raviraj, Tejas: *QCA design and implementation of SRAM based FPGA configurable logic block*, Circuits and Systems (MWSCAS), 2010 53rd IEEE International Midwest Symposium on, pag. 837-840, IEEE. 4

[6] Erlagen Numberg University: *Quantum Dot Cellular Automata*, 2012. 2, 3

[7] Cho, Heumpil and Swartzlander Jr., Earl E.: *Adder and multiplier design in quantum-dot cellular automata*, IEEE Transactions on Computers, vol. 58, n. 6, pag. 721-727, 2009, IEEE. 4, 6

[8] Walus, Konrad and Jullien, Graham A: *Design tools for an emerging SoC technology: Quantum-dot cellular automata*, Proceedings of the IEEE, vol. 94, n. 6, pag. 1225-1244, 2006, IEEE. 5

[9] Sridharan, Krishnamurthy and Pudi, Vikramkumar: *Design of Arithmetic Circuits in Quantum Dot Cellular Automata Nanotechnology*, 2016, Springer. 5

[10] Pickover, Clifford A.: *The math book: from Pythagoras to the 57th dimension, 250 milestones in the history of mathematics*, 2009, Sterling Publishing Company, Inc. 6

[11] Lent, Craig S and Isaksen, Beth and Lieberman, Marya: *Molecular quantum-dot cellular automata*, Journal of the American Chemical Society, vol. 125, n. 4, pag. 1056-1063, 2003, ACS Publications. 6

[12] Snider, Gregory L and Orlov, Alexei O and Kummamuru, Ravi K and Ramasubramaniam, Rajagopal and Amlani, Islamshah and Bernstein, Gary H and Lent, Craig S:

Quantum-dot cellular automata, MRS Online Proceedings Library Archive, vol. 696, 2001, Cambridge University Press. 6

[13] Leonardo Doffo: *Analysis and development of a structure for nanocomputing based on organic molecules*, Master Degree Thesis, pag.9, 2016, Polytechnic of Turin. 7

[14] Wang, Ruiyu and Pulimeno, Azzurra and Roch, Massimo Ruo and Turvani, Giovanna and Piccinini, Gianluca and Graziano, Mariagrazia: *Effect of a clock system on bis-ferrocene molecular QCA*, IEEE Transactions on Nanotechnology, vol. 15 , n. 4, pag. 574-582, 2016, IEEE. 7, 12, 13

[15] Qi, Hua and Sharma, Sharad and Li, Zhaohui and Snider, Gregory L and Orlov, Alexei O and Lent, Craig S and Fehlner, Thomas P: *Molecular quantum cellular automata cells. Electric field driven switching of a silicon surface bound array of vertically oriented two-dot molecular quantum cellular automata*, Journal of the American Chemical Society, vol. 125, n. 49, pag. 15250-15259, 2003, ACS Publications. 7

[16] Zaker, Evan: *Nano-fabrication of Accommodative Intraocular Lenses Using Gray-scale Electron Beam and Soft Lithography*, Master Thesis, University of Illinois at Chicago, 2012. 17

[17] Bernstein, Gary H and Imre, Alexandra and Metlushko, V and Orlov, A and Zhou, L and Ji, L and Csaba, György and Porod, Wolfgang: *Magnetic QCA systems*, Microelectronics Journal, volume 36, n. 7, pag. 619-624, 2005, Elsevier. 8

[18] Cofano, M and Santoro, Giulia and Vacca, Marco and Pala, D and Causapruno, Giovanni and Cairo, Fabrizio and Riente, Fabrizio and Turvani, Giovanna and Roch, M Ruo and Graziano, Mariagrazia and others: *Logic-in-memory: A nano magnet logic implementation*, VLSI (ISVLSI), 2015 IEEE Computer Society Annual Symposium on,pag. 286-291, 2015, IEEE. 9, 10

[19] Bhanja, Sanjukta and Pulecio, Javier: *A review of magnetic cellular automata systems*, Circuits and Systems (ISCAS), 2011 IEEE International Symposium on, pag. 2373-2376, 2011, IEEE. 10

[20] Lorenzo Polsinelli: *Simulation of nanoelectronic systems: molecular QCA circuits*, Master Degree Thesis, pag. 8-12, Polytechnic of Turin, 2016-2017. 14

[21] Mølhave, Kristian and Madsen, Dorte Nørgaard and Bøggild, Peter: *A simple electron-beam lithography system*, Ultramicroscopy, volume 102, n. 3, pag. 215-219, year 2005, Elsevier. 16

[22] Davisson, Clinton and Germer, Lester Halbert: *The scattering of electrons by a single crystal of nickel*, Nature , volume 119, n. 2998, pag. 558, 1927, Nature Publishing Group. 16

[23] Mohammad, Mohammad Ali and Muhammad, Mustafa and Dew, Steven K and Stepanova, Maria: *Fundamentals of electron beam exposure and development*, Nanofabrication, pag. 11-41, 2012 Springer. 17, 18

[24] De Broglie, Louis: *The wave nature of the electron*, Nobel lecture, vol. 12, pag. 244-256, 1929. 18

[25] Goldstein, Joseph I and Newbury, Dale E and Michael, Joseph R and Ritchie, Nicholas WM and Scott, John Henry J and Joy, David C: *Scanning electron microscopy and X-ray microanalysis*, 2017, Springer. 18

[26] Lundstrom, Torsten: *Structure, defects and properties of some refractory borides*, Pure and Applied Chemistry, vol. 57, n. 10, pag. 1383-1390, year 1985. 18

[27] Williams, David B and Carter, C Barry: *The transmission electron microscope*, Transmission electron microscopy, pag. 3–17, 1996, Springer. 19

[28] De Jonge, Niels and Bonard, Jean–Marc: *Carbon nanotube electron sources and applications*, Philosophical Transactions of the Royal Society of London A: Mathematical, Physical and Engineering Sciences, vol. 362, n. 1823, pag. 2239-2266, 2004, The Royal Society. 19

[29] Rai-Choudhury, Prosenjit: *Handbook of microlithography, micromachining, and microfabrication: microlithography*, vol. 1, 1997, Iet. 21, 30

[30] Zheng, Cui: *Nanofabrication: principles, capabilities and limits*, Springer, Germany, 2008. 21

[31] Gusman, Andrea and Chandu, Srivigyan and Yaghmaie, Frank: *ZEP520A–New resist for Electron Beam Lithography*, 2011, tech. rep., Available at: http://research. engineering. ucdavis. edu/cnm2/wpcontent/uploads/sites/11/2013/05/ZEP520A-Process.pdf. 25

[32] Zheng, Ai Zhi: *A Developer-free Approach to Conventional Electron Beam Lithography*, 2012. 21, 24

[33] Microchem: *PMMA Data-sheet*, 1254 Chestnut St., Newton. 24, 25

[34] Grigorescu, AE and Hagen, CW: *Resists for sub-20-nm electron beam lithography with a focus on HSQ: state of the art*, Nanotechnology, vol. 20, n. 29, pag. 292001, 2009, IOP Publishing. 25

[35] Abhay Kotnala: *Proximity Effect in EBL*, Electrical and Computer Engineering Department, University of Victoria. 26

[36] Egerton, RF and Li, P and Malac, M: *Radiation damage in the TEM and SEM*, Micron,vol. 35, n. 6, pag. 399-409, 2004, Elsevier. 26, 27

[37] Cabrini, Stefano and Kawata, Satoshi: *Nanofabrication handbook*, 2012, CRC Press. 27

[38] Elsner, H and Meyer, H-G: *Nanometer and high aspect ratio patterning by electron beam lithography using a simple DUV negative tone resist*, Microelectronic engineering, vol. 57, pag. 291-296, 2001, Elsevier. 31

[39] Li, Pengcheng: *A Review of Proximity Effect Correction in Electron-beam Lithography*, arXiv preprint arXiv:1509.05169, 2015. 32

[40] Phang, JCH and Ahmed, H: *Line profiles in thick electron resist layers and proximity effect correction*, Journal of Vacuum Science and Technology, vol. 16, n. 6, pag. 1754-1758, 1979, AVS. 32, 33

[41] Dobisz, Elizabeth A and Marrian, Christie R and Salvino, RE and Ancona, Mario G and Rhee, Kee Woo and Peckerar, Martin C: *Thin silicon nitride films to increase resolution in e-beam lithography*, Optical Engineering, vol. 32, n. 10, pag. 2452-2459, 1993, International Society for Optics and Photonics. 34

[42] Kovacs, Gregory TA and Maluf, Nadim I and Petersen, Kurt E: *Bulk micromachining of silicon*, Proceedings of the IEEE, vol. 86, n. 8, pag. 1536-1551, 1998, IEEE. 37

[43] Harsha, KSKS Sree: *Principles of vapor deposition of thin films*, 2005, Elsevier. 41

[44] Green, TA: *Gold etching for microfabrication*, Gold Bulletin, vol. 47, n. 3, pag. 205-216, 2014, Springer. 41

[45] Williams, Kirt R and Gupta, Kishan and Wasilik, Matthew: *Etch rates for micromachining processing-Part II*, Journal of microelectromechanical systems, vol. 12, n. 6, pag. 761-778, 2003, IEEE. 43

[46] Halverson, RM and MacIntyre, MW and Motsiff, WT: *The mechanism of single-step liftoff with chlorobenzene in a diazo-type resist*, IBM Journal of Research and Development, vol. 26, n. 5, 590-595, 1982, IBM. 44

[47] Ruska, Ernst: *The early development of electron lenses and electron microscopy*,Microscopica acta. Supplement, n. 5, pag. 1-140, 1980. 48

[48] Orloff, Jon: *Charged Particle Optics*, 2009, Wiley Online Library. 50

[49] Hawkes, PW: *The correction of electron lens aberrations*, Ultramicroscopy, vol. 156, pag. A1-A64, 2015, Elsevier. 52

[50] Pennycook, SJ and Jesson, DE: *High-resolution Z-contrast imaging of crystals*, Ultramicroscopy, vol. 37, n. 1-4, pag. 14-38, 1991, Elsevier. 50

[51] Elsass, FRANÇOISE and Chenu, CLAIRE and Tessier, DANIEL and Ulery, AL and Drees, LR: *Transmission electron microscopy for soil samples: preparation methods and use*, Methods of Soil Analysis. Part, vol. 5, pag. 235-267, 2008. 54

[52] Zhang, Xiao Feng and Kamino, Takeo: *Imaging gas-solid interactions in an atomic resolution environmental TEM*, Microsc. Today, vol. 14, pag. 16, 2006. 56